Journal for ImmunoTherapy of Cancer

Adenovirus vaccine targeting kinases induces potent antitumor immunity in solid tumors

Fei Zhu,[1,2,3] Zheng Lu,[1,2,3] Wenjing Tang,[4] Guangya Zhao,[1,2,3] Yingxiang Shao,[1,2,3] Bowen Lu,[1,2,3] Jiage Ding,[5] Yanyan Zheng,[1,2,3] Lin Fang,[1,2,3] Huizhong Li,[1,2,3] Gang Wang ,[1,2,3] Renjin Chen,[6] Junnian Zheng ,[2,3] Dafei Chai [1,3,7]

To cite: Zhu F, Lu Z, Tang W, *et al*. Adenovirus vaccine targeting kinases induces potent antitumor immunity in solid tumors. *Journal for ImmunoTherapy of Cancer* 2024;**12**:e009869. doi:10.1136/jitc-2024-009869

► Additional supplemental material is published online only. To view, please visit the journal online (https://doi.org/10.1136/jitc-2024-009869).

FZ and ZL contributed equally.

Accepted 12 August 2024

For numbered affiliations see end of article.

Correspondence to
Dr Dafei Chai;
chaidafei@xzhmu.edu.cn

Dr Junnian Zheng;
jnzheng@xzhmu.edu.cn

Renjin Chen; crj@xzhmu.edu.cn

ABSTRACT

Background Targeting kinases presents a potential strategy for treating solid tumors; however, the therapeutic potential of vaccines targeting kinases remains uncertain.

Methods Adenovirus (Ad) vaccines encoding Aurora kinase A (AURKA) or cyclin-dependent kinase 7 (CDK7) were developed, and their therapeutic potentials were investigated by various methods including western blot, flow cytometry, cytotoxic T lymphocyte assay, and enzyme-linked immunospot (ELISpot), in mouse and humanized solid tumor models.

Results Co-immunization with Ad-AURKA/CDK7 effectively prevented subcutaneous tumor growth in the Renca, RM-1, MC38, and Hepa1-6 tumor models. In therapeutic tumor models, Ad-AURKA/CDK7 treatment impeded tumor growth and increased immune cell infiltration. Administration of Ad-AURKA/CDK7 promoted the induction and maturation of dendritic cell subsets and augmented multifunctional $CD8^+$ T-cell antitumor immunity. Furthermore, the vaccine induced a long-lasting antitumor effect by promoting the generation of memory $CD8^+$ T cells. Tumor recovery on $CD8^+$ T-cell depletion underscored the indispensable role of these cells in the observed therapeutic effects. The potent efficacy of the Ad-AURKA/CDK7 vaccine was consistently demonstrated in lung metastasis, orthotopic, and humanized tumor models by inducing multifunctional $CD8^+$ T-cell antitumor immune responses.

Conclusions Our findings illustrate that the Ad-AURKA/CDK7 vaccine targeting dual kinases AURKA and CDK7 emerges as a promising and effective therapeutic approach for the treatment of solid tumors.

WHAT IS ALREADY KNOWN ON THIS TOPIC

⇒ Kinases play a critical role in cancer cell survival and proliferation, making them potential targets for cancer therapy. Traditional treatments targeting kinases include small molecule inhibitors, but vaccines targeting kinases have not been extensively studied for their therapeutic potential against solid tumors.

WHAT THIS STUDY ADDS

⇒ In this study, we develop adenovirus vaccines encoding Aurora kinase A (AURKA) or cyclin-dependent kinase 7 (CDK7) and demonstrate their potent therapeutic effects in multiple tumor models. Adenovirus-AURKA/CDK7 co-immunization enhances immune cell infiltration, promotes the induction and maturation of dendritic cell subsets, and augments multifunctional $CD8^+$ T-cell antitumor immunity. The vaccine induces a long-lasting antitumor effect by generating memory $CD8^+$ T cells, with the indispensable role of $CD8^+$ T cells confirmed by tumor recovery on their depletion.

HOW THIS STUDY MIGHT AFFECT RESEARCH, PRACTICE OR POLICY

⇒ Our study highlights the potential of kinase-targeting vaccines, particularly those targeting AURKA and CDK7, as effective therapeutic strategies for solid tumors. It provides a basis for further research into vaccine-based approaches for cancer treatment, potentially leading to new vaccine therapies targeting other kinases. Our study promotes clinical practices by introducing new immunotherapeutic options and guiding vaccine development strategies for solid tumors.

INTRODUCTION

Solid tumors frequently exhibit an increased susceptibility to evasion, recurrence, and metastasis, ultimately leading to patient mortality.[1] However, conventional therapeutic modalities such as surgery, radiotherapy, and chemotherapy have proven to be only partially effective.[2–4] Immunotherapy, an advanced approach to cancer treatment, activates the body's immune system to efficiently recognize and destroy cancer cells. This encompasses the use of checkpoint inhibitor, cellular immunotherapy, oncolytic virus, and cancer vaccine.[5–8] Recent advancements in immunotherapy have highlighted the essential role of cancer vaccines in eliciting immune responses and hindering tumor growth.[9]

Cancer vaccine represents a promising immunotherapeutic strategy that augments the cytotoxicity of tumor-specific $CD8^+$ T cells and elicits innate immune responses.[10 11]

Studies have shown the potential of vaccines in inducing the regression of substantial tumors and prolonging survival time.[12–14] Notably, for enhanced immunogenicity and safety, an adenovirus (Ad) vaccine is chosen to amplify the immune response against the encoded antigens.[15 16] Additionally, owing to its high infectivity and low toxicity, Ad has been used for gene delivery or as a carrier for vaccination.[17] Importantly, replication-deficient Ads equipped with robust exogenous promoters could significantly enhance the delivery of the target antigens. Furthermore, the absence of essential E1 genes in replication-deficient Ad contributes to improving safety and reducing side effects.[18–20]

Universally acknowledged, the selection of appropriate tumor antigens that effectively activate tumor-specific immune responses is crucial for enhancing antitumor efficacy and specific killing.[21–23] Aurora kinase A (AURKA), a serine/threonine kinase family, regulates cell mitosis and is essential for the proliferation and metastasis of tumor cells.[24] The expression of activated AURKA is significantly elevated in various solid tumor types compared with that in normal control tissues.[25] Expressing an AURKA-specific T-cell receptor retained sensitivity and efficacy against AURKA-positive acute myeloid leukemia cells.[26] Aurora-A kinase's 9-amino-acid epitope induces specific cytotoxic T lymphocytes (CTLs) to target human leukemia and $CD34^+$ hematopoietic stem cells, but not normal cells.[27 28] Moreover, several studies have suggested that inhibitors targeting AURKA may slow the growth of multiple tumors, making AURKA a viable target for suppressing tumor growth.[29–31]

Cyclin-dependent kinase 7 (CDK7), as a member of the serine/threonine kinase family, signifies the dependence of transcriptional addition in cancers, playing a crucial role in regulating cell cycle and gene transcription.[32–35] Inhibition of CDK7 has been demonstrated to significantly suppress various types of solid tumors and remarkably prolong survival time.[36–38] Due to its elevated expression in tumors, such as human renal cell carcinoma and prostate cancer.[39 40] CDK7 is considered an emerging prognostic biomarker and therapeutic target.[34 41 42] Despite the promising therapeutic effects demonstrated by kinase inhibitors on solid tumors, safety concerns, such as drug resistance or severe side effects have hindered their clinical applicability.[43] So, there is an urgent need to develop new therapeutic methods targeting AURKA and CDK7 kinases to treat solid tumors with low toxicity.

In this study, we developed a replication-deficient Ad vaccine that encoded either AURKA or CDK7. The therapeutic efficacy of the combined Ad-AURKA/CDK7 vaccines was observed in prophylactic and therapeutic tumor models. Our findings revealed that the Ad-AURKA/CDK7 vaccine effectively promoted the induction and maturation of dendritic cells (DCs) and notably activated the antitumor response of $CD8^+$ T cells, thereby hindering the progression of solid tumors in the combined group. The infiltration capacity of $CD8^+$ T cells into tumors, along with the secretion of interferon (IFN)-γ, tumor necrosis (TNF)-α, or interleukin (IL)-2 cytokines by multifunctional $CD8^+$ T cells, showed a significant increase in the combined immunotherapy. This phenomenon was consistently observed in all four models (subcutaneous, lung metastatic, orthotopic, and humanized tumor models). In conclusion, a novel vaccine strategy targeting dual kinases AURKA and CDK7 demonstrated favorable therapeutic effects, providing a promising approach for overcoming solid tumors.

METHODS

Animals

BALB/c, C57L, C57BL/6 wild-type mice (female or male) aged 6–8 weeks old, and $CD34^+$ humanized HLA-transgenic NOD.Cg-Prkdc^{scid} Il2rg^{tm1Wjl}/SzJ (NSG) mice aged approximately 15 weeks old were obtained from the Laboratory Animal Center of Xuzhou Medical University. Humanized mice were prepared by injecting human hematopoietic stem cells isolated from human umbilical cord blood into the liver of newborn HLA-transgenic NSG mice that had received 100 cGy total body irradiation within 3 days of birth. These mice were housed under specific pathogen-free conditions with standard humidity and temperature. All procedures and animal experimental protocols were approved by the Laboratory Animal Ethics Committee of Xuzhou Medical University (reference number: 202405T023). The guidelines for the Care and Use of Laboratory Animals of Xuzhou Medical University were strictly followed, and all codes of conduct were duly observed.

Cell culture

The Human Embryonic Kidney 293 (HEK-293), mouse Hepa1-6, and RM-1 cell lines were purchased from the American Type Culture Collection and cultured in a DMEM medium (Gibco, Invitrogen). The Renca cell line was obtained from Cobioer Biosciences (Nanjing, China) and maintained in RPMI-1640 medium (Gibco, Invitrogen) supplementing with 1×non-essential amino acid solution (NEAAS, Sigma), 1×sodium pyruvate (Sigma) and 1×L-glutamine (L-Glu, Sigma). The Hepa1-6 cell line was cultured in a DMEM medium containing 1×NEAAS, 1×L Glu, and 1×sodium pyruvate. The MC38 cell line was obtained from Cell Resource Center, IBMS, CAMS/PUMC (Beijing, China), and cultured in DMEM medium maintaining 1×NEAAS. Human renal carcinoma cell line OSRC-2 was purchased from the Chinese Academy of Sciences (Shanghai, China) and cultured in RPMI-1640 medium (Gibco, Invitrogen). In addition to providing extra nutrients, all culture media required the addition of 10% fetal bovine serum (ExCell Bio) and 1×penicillin-streptomycin. All the cells were cultured at 37°C in a humidified incubator with 5% CO_2.

Preparation of Ad vaccine

Two types of vectors for packaging viruses, shuttle vector pDC315, and E1A-absent Ad5 backbone vector pPE3, were

gifted by Professor Lin Fang of Xuzhou Medical University. Gene-targeted fragments of AURKA or CDK7 were amplified from pCMV-AURKA-SV40-Neo (Miaoling Bio) or pCMV-CDK7-SV40-Neo (Miaoling Bio). The AURKA fragment was subcloned into the pDC315 vector to form pDC315-AURKA using BamH I and Sal I sites, while the CDK7 fragment was subcloned using EcoR I and BamH I sites to form pDC315-CDK7. To determine their current structures, pDC315-AURKA and pDC315-CDK7 were sequenced. Then, using homologous recombination methods, they were co-transfected into HEK-293 cells with pPE3 to produce Ad-AURKA and Ad-CDK7, along with control Ad (Ad-Ctrl). Viral plaques were formed approximately 12–15 days after transfection. Ads were purified using ultracentrifugation with cesium chloride. The titers were confirmed using the TCID50 assay. Simultaneously, to explore whether combination therapy with AURKA and CDK7 could promote antitumor effects against human renal carcinoma, human Ad-AURKA (Ad-hAURKA) was constructed using the same method, and Ad-CDK7 was continued to be used because of its homology between humans and mice.

To package Ad vaccines, the shuttle plasmids and the E1A-deleted type 5 backbone vector pPE3 were mixed, and then co-transfected into the HEK-293 cell line for homologous recombination. When plaques were visible, the supernatant of the culture was centrifuged and DNA was extracted using the QIAGEN genomic DNA kit. DNA amplification was performed by PCR with primers specific for AURKA or CDK7. Subsequently, DNA purity was assessed by electrophoresis on 1.5% agarose gels for 35 min at 110 V. The gels were analyzed using the Tanon Gel Image System (Tanon) at a wavelength of 312 nm.

Western blot

Tissues were lysed to obtain soluble protein samples. Subsequently, they were separated by 12% sodium dodecyl sulfate-polyacrylamide gel electrophoresis and transferred onto polyvinylidene fluoride membranes. After blocking with 5% skim milk at room temperature for 1 hour, the membranes were incubated overnight at 4°C with primary antibodies targeting AURKA (Proteintech, Cat# 66757–1-Ig) or CDK7 (Proteintech, Cat# 27027–1-AP). Next, they were washed thrice with Tris buffered saline containing Tween-20 and then incubated with a secondary antibody for 2 hours at room temperature. Ultimately, after three consecutive washes, western blot bands were visualized using enhanced chemiluminescence (Thermo Fisher Scientific).

Animal models and immunizations

For the prophylactic tumor models, Ad-Ctrl or Ad-AURKA/CDK7 was intramuscularly administered into the right thigh of the mice on days −7 to −17, and −27. Subsequently, the corresponding number of tumor cells, suspended in 100 µL phosphate-buffered saline (PBS) (Renca, 5×10^5 cells per mouse; RM-1, 5×10^5 cells per mouse; Hepa1-6, 2×10^6 cells per mouse; MC38, 1×10^6 cells per mouse), was subcutaneously implanted on the same flank of the mice's back on day 0. Mice were immunized with Ad-Ctrl, Ad-AURKA, Ad-CDK7 at a dose of 3×10^8 plaque forming units (PFU) each vaccine one time, and Ad-AURKA/CDK7 at a dose of 6×10^8 PFU. For the Ad-Ctrl, Ad-AURKA, and Ad-CDK7 immunized group, mice received an additional 3×10^8 PFU Ad-Ctrl to ensure that the total Ad vaccine amount was the same. Tumors were assessed using the following formula to estimate the tumor volumes: V (mm^3)=(length×width×width)/2. On reaching a specific volume, the mice were euthanized and tumor weights were recorded. For the treatment of therapeutic tumor models, mice were intramuscularly immunized with Ad vaccines on days 7, 17, and 27 after subcutaneous inoculation of Renca cells on day 0. For the lung metastasis model, 5×10^5 Renca cells were intravenously injected on day 0, and the mice received Ad vaccines on days 1, 8, and 15 post-tumor inoculation. The lungs were surgically excised, and metastatic nodules in the lung tissues were quantified. In the orthotopic tumor model, under anesthesia, 1×10^5 Renca cells suspended in 10 µL were injected into the left kidney, and each layer of the wound was sutured. The vaccination procedure mirrored that in the lung model. For the humanized mice model, OSRC-2 renal carcinoma cells were subcutaneously implanted on day 0, followed by intramuscular vaccination with various treatments on days 7, 17, and 27. The formula for calculating the tumor mass in the orthotopic model was as follows: Tumor mass (g)=left kidney mass − right kidney mass.

For the tumor rechallenge experiment, vaccine-immunized mice underwent surgical excision of the primary tumor and were then subcutaneously re-challenged with 5×10^5 Renca cells on the contralateral side. Naive mice without tumors served as the control group.

Flow cytometry detection

Tumor tissues and spleens were gently homogenized to release the cells. Debris was removed by filtering through 70 µm filter screens into centrifuge tubes and centrifuged at 2,000×rpm for 5 min. Then, red blood cells in the gathered cell suspension were lysed using an ACK lysis buffer. The remaining cells from tumor tissues were centrifuged to isolate tumor-infiltrating leukocytes (TILs) using the 33.3% Percoll (VicMed) gradient method. This process was employed to prepare single-cell suspensions for culturing or staining.

For the staining of single-cell surfaces, the following flow cytometry antibodies were used: anti-mouse CD11c (APC, BioLegend, Cat# 117310), anti-human/mouse CD11b (FITC, BioLegend, Cat# 101206), anti-muse CD3ε (PE, BioLegend, Cat# 100308), anti-mouse CD4 (PerCP-Cy5.5, BioLegend, Cat# 116012), anti-mouse CD8α (PerCP-Cy5.5, BioLegend, Cat# 100734), anti-mouse CD80 (PE, BioLegend, Cat# 104708), anti-mouse CD86 (PE, BioLegend, Cat# 159204), anti-mouse MHC-II (PE, BioLegend, Cat# 107608), anti-mouse CD40 (PE, BioLegend, Cat# 157506), anti-mouse Gr-1

(PerCP-Cy5.5, BioLegend, Cat# 108426), anti-mouse CD45 (PE-Cy7, BioLegend, Cat# 103114), anti-mouse CD49b (FITC, BioLegend, Cat# 108906), anti-mouse NK1.1 (FITC, BioLegend, Cat# 108706), anti-mouse F4/80 (PerCP, BioLegend, Cat# 123126), anti-mouse CD44 (PE, BioLegend, Cat# 103008), anti-mouse CD62L (APC, BioLegend, Cat# 104412), anti-human CD45 (APC-Cy7, BioLegend, Cat# 304014), anti-human CD8α (PerCP-Cy5.5, BioLegend, Cat# 301032), anti-human CD11c (APC, BioLegend, Cat# 301614), anti-human CD103 (PE, BioLegend, Cat# 350206), anti-human CD80 (PE, BioLegend, Cat# 305208), anti-human CD86 (FITC, BioLegend, Cat# 374204), anti-human HLA-DR (Pacific Blue, BioLegend, Cat# 307624), anti-human HLA-A2 (PerCP-Cy5.5, BioLegend, Cat# 343316), and DAPI (BioLegend, Cat# 422801). Cells were thoroughly mixed with antibodies, and the mixture was incubated at 4°C for 1 hour. Subsequently, cells were washed twice with PBS.

For the staining of intracellular cytokines, 5×10^6 spleen cells were resuspended in each 12-well plate and stimulated with AURKA/CDK7 antigens (purified from the HEK293 cell expression system) for 72 hours. Cells were constantly stimulated for 5 hours in a cell incubator with 5 µg/mL brefeldin A (eBioscience), 50 ng/mL PMA (Sigma-Aldrich) and 500 ng/mL lonomycin (Sigma-Aldrich). The obtained cells were washed with PBS and stained with anti-mouse CD8α (PerCP-Cy5.5, BioLegend, Cat# 100734) and anti-mouse CD45 (PE-Cy7, BioLegend, Cat# 103114) for 1 hour, followed by intracellular staining overnight with anti-mouse TNF-α (Alexa Fluor 488, BioLegend, Cat# 506313), anti-mouse IFN-γ (APC, BioLegend, Cat# 505810), and anti-mouse IL-2 (PE, BioLegend, Cat# 503808). Meanwhile, human flow cytometry antibodies were used: anti-human IL-2 (PE, BioLegend, Cat# 500307), anti-human TNF-α (Alexa Fluor 488, BioLegend, Cat# 502915), and anti-human IFN-γ (APC, BioLegend, Cat# 506510). Finally, the cells were washed twice with PBS.

CD8$^+$ T-cell proliferation

Lymphocytes were cultured in the medium containing IL-2 (50 U/mL) and AURKA/CDK7 antigens (10 µg/mL), and then inoculated into 48-well flat plates at a density of 1×10^6 cells per well. The plates were placed in a constant temperature incubator at 37°C for 4–6 days, with a medium change on day 3. Proliferation was assessed using the BeyoClick EdU Cell Proliferation Kit (Alexa Fluor 647, Beyotime). Specifically, the cells were incubated with 10 µM EdU at 37°C for 2 hours, followed by centrifugation and staining with anti-mouse CD8α (PerCP-Cy5.5, BioLegend, Cat# 100734) for 30 min. After fixation, permeabilization, and rinsing, the lymphocytes were treated with the click reaction cocktail for 1 hour at room temperature. Finally, the cells were washed with the permeabilization buffer and resuspended in PBS. The proportion of EdU$^+$ in CD8$^+$ T cells was analyzed by flow cytometry.

Cytotoxic T lymphocyte assay

As effector cells, lymphocytes were cultured in the medium supplemented with IL-2 (50 U/mL) and AURKA/CDK7 antigens (10 µg/mL) at 37°C in a humidified incubator containing 5% CO_2 for 5 days, with a half-volume medium change on day 3. GFP-Renca cells, which served as target cells, expressed green fluorescence. After co-culturing effector cells (3×10^6/well) with target cells (2×10^5 cells/well) for 2 days in 24-well plates in a culture incubator with 5% CO_2, the cells were collected and stained with anti-mouse CD8α (PerCP-Cy5.5, BioLegend, Cat# 100734). Subsequently, data were obtained using flow cytometry, and the CTL effects were calculated based on the ratio of killed target cells.

ELISpot assay

Mouse T cells expressing IFN-γ were detected using a mouse IFN-γ single-color enzymatic ELISpot kit (ImmunoSpot, Cat# SKU: mIFNgp-1M). Initially, the enzyme-linked immunospot (ELISpot) plates were treated with 70% ethanol, washed with PBS, and subsequently coated with IFN-γ capture solution (ImmunoSpot) overnight at 4°C. The plates were then washed and incubated with CTL-Test Medium containing AURKA/CDK7 antigens at 37°C in a CO_2 incubator. Additionally, 5×10^5 lymphocytes per well were inoculated into the plates and cultured in a humidified incubator at 37°C for 3 days. Following incubation with the IFN-γ detection antibody, the sample underwent enzyme-catalyzed substrate precipitation (ImmunoSpot), resulting in color formation. Finally, the results were analyzed by an ImmunoSpot S6 Ultimate Reader from CTL, and the spot-forming cells were quantified using the ImmunoSpot software (CTL).

CD8$^+$ T-cell depletion in vivo

For depletion of CD8$^+$ T cells in vivo, mice received intraperitoneal injections of 0.5 mg anti-mouse CD8α monoclonal antibody (mAb, Bio X Cell, Cat# BE0061) per mouse 2 days prior to the initial immunization. The mAb was administered again on days 5 and 12. To assess the efficacy of CD8$^+$ T-cell depletion, spleen cells were processed into single-cell suspensions for flow cytometric analysis.

Immunohistochemical and H&E staining

Immunohistochemical (IHC) staining was performed on tumor sections that were fixed with formalin, embedded in paraffin and sectioned into 5 µm slices. Subsequently, the sections were heated in 10 mM sodium citrate (PH 6.0) for 30 min, followed by incubation with 3% hydrogen peroxide for 1 hour. Tissues were blocked with 10% bovine serum albumin for 2 hours, and then incubated sequentially with rat anti-mouse CD8α antibody (eBioscience, Cat# 14-0081-82; diluted 1:100) and goat anti-rat antibody (Zhongshan Bio-Tech). Nuclei were counterstained with hematoxylin. Finally, the tumor sections were developed using a DAB detection kit (Zhongshan Bio-Tech). Simultaneously, Hematoxylin and eosin (H&E) staining

of the heart, lung, liver, and kidney tissues was performed according to the provided instructions. Sections from each group were blindly evaluated by a pathologist, and images were captured using an Olympus IX73 microscope (Olympus) with CellSens Entry software at a scale of 200 µm.

Statistical analyses

Data were presented as mean and SD (mean±SD). Statistical analysis was performed using the GraphPad Prism V.9.0 software. The two-tailed independent Student's t-test was used to analyze two-group comparisons. For multiple group comparisons, one-way analysis of variance (one-way analysis of variance) was employed. Survival analysis was performed using the log-rank (Mantel-Cox) test. The statistical significance levels were denoted as follows: *p<0.05, **p<0.01, ***p<0.001, and ****p<0.0001.

RESULTS

Ad-AURKA/CDK7 immunization prevents tumor growth in various solid tumor models

Ad-AURKA or Ad-CDK7 was prepared as described in the Methods section. Confirmation of correct Ad packaging was obtained when the plaque was visible, as verified by western blot and viral gene PCR (online supplemental figure S1). These results indicated the successful and efficient expression of targeted genes coded by Ad vaccines.

Previous studies showed the high expression of AURKA and CDK7 in various cancers, including renal cell carcinoma, prostate cancer, liver cancer, and colorectal cancer.[38 44–48] Building on this, elevated expression of AURKA and CDK7 was observed in Renca, MC38, RM-1, and Hepa1-6 (online supplemental figure S2). Subsequently, 6–8 weeks old mice were randomly divided into two groups, with each group receiving intramuscular immunization with Ad-Ctrl or Ad-AURKA/CDK7 on days 7, 17, and 27 before tumor cells implantation on day 0 (figure 1A). Compared with the Ad-Ctrl group, Ad-AURKA/CDK7 immunization effectively inhibited tumor growth in Renca, MC38, RM-1, and Hepa1-6 subcutaneous tumor models (figure 1B,F,J,N), and the tumor volume curves of each mouse in the combined groups were significantly suppressed (figure 1C,G,K,O). Next, the final tumor weights in the Ad-AURKA/CDK7 group were noticeably lower than those in the Ad-Ctrl group (figure 1D,H,L,P). Similarly, the tumor inhibition rates were higher in the Ad-AURKA/CDK7 co-immunization group. When comparing the tumor inhibition rates in other tumor models, the Renca group exhibited the highest inhibition proportion and the most effective prevention after the vaccine immunization (figure 1E,I,M,Q). These results suggested that Ad-AURKA/CDK7 co-immunization effectively prevented the growth of Renca, MC38, RM-1, and Hepa1-6 tumors, with the strongest preventive effect observed in the Renca tumor model.

Ad-AURKA/CDK7 treatment suppresses tumor growth and enhances the tumor-infiltrating immune cells in the Renca subcutaneous model

Owing to the highest tumor inhibition rate and the most effective preventive effect, the Renca tumor model was chosen to investigate the effectiveness of subcutaneous tumors in the treatment models. To investigate the antitumor effect of Ad-AURKA/CDK7 in vivo, 5×10^5 Renca cells were subcutaneously implanted on day 0. Seven days after tumor inoculation, mice were randomly divided into four groups and intramuscularly immunized with Ad-Ctrl, Ad-AURKA, Ad-CDK7, and Ad-AURKA/CDK7 on days 7, 17, and 27. Moreover, each group of mice served a dual purpose: some were used to assess tumor growth and detect immune cells in spleens and tumors, while others were re-challenged with Renca tumors to explore the sustained maintenance of antitumor effects. Tumor volumes and weights were monitored as described in the prophylactic model (figure 2A). At the end of the experiment, compared with the Ad-CDK7 single vaccine group, tumor volumes in the Ad-AURKA/CDK7 group were significantly inhibited (figure 2B,C). It was equally significant that mice in the combined immunization group had lower tumor weights and higher inhibition rates than those in the Ad-AURKA or Ad-CDK7 groups (figure 2D,E). For the safety evaluation of the vaccine, our results showed that no significant difference was observed in the proliferation of Renca cells infected with Ad-AURKA/CDK7 compared with other Ads (online supplemental figure S3). H&E staining confirmed that Ad vaccines did not induce abnormal pathological changes in the heart, kidney, lung, and liver tissues (online supplemental figure S4).

Furthermore, our results showed that the preventive Ad-AURKA/CDK7 vaccine induced higher serum titers of IgG antibodies against the AURKA or CDK7 antigens, whereas the therapeutic Ad-AURKA/CDK7 vaccine induced significantly lower titers (online supplemental figure S5). Moreover, the therapeutic vaccine of Ad-AURKA or Ad-CDK7 cannot efficiently prevent tumor growth in the subcutaneous tumor model, suggesting that the antibody-mediated immune responses did not effectively eliminate the tumors. To elucidate the potential mechanism underlying the tumor inhibition effects of the Ad-AURKA/CDK7 vaccine, flow cytometry data revealed varying proportions of immune cells infiltrating subcutaneous tumors, explaining the antitumor therapy results. As anticipated, compared with the Ad-AURKA or Ad-CDK7 treatment groups, the ratios of total tumor-infiltrating T cells, $CD8^+$ T cells, and DCs were elevated in the combination group, and this phenomenon was observed in both spleens and tumors (figure 2F,G). Additionally, the data also indicated that the proportions of natural killer (NK) cells, $CD4^+$ T cells, and macrophages (Mϕ) did not exhibit significant differences in each

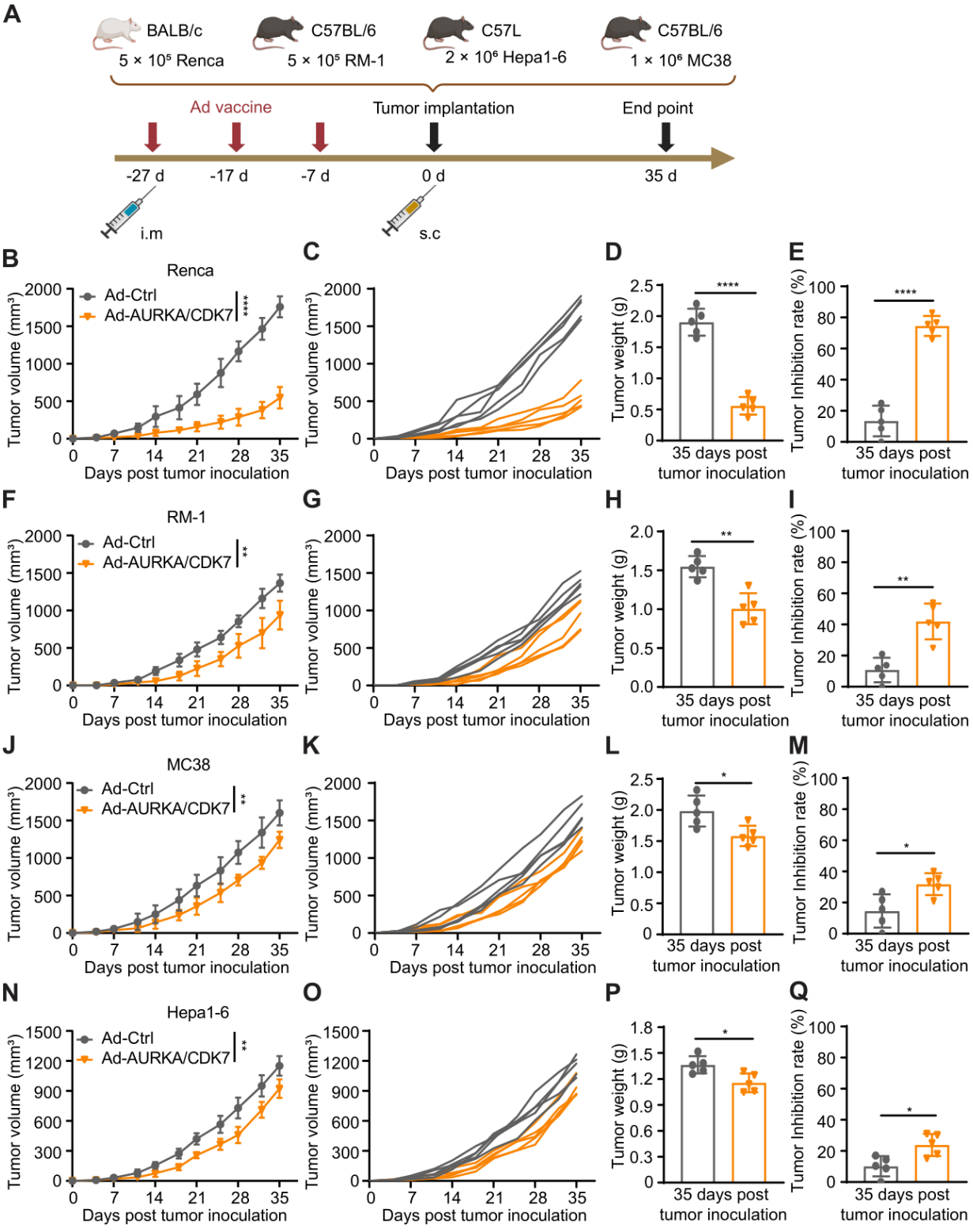

Figure 1 The protective efficacy of the Ad-AURKA/CDK7 vaccine on various tumors in the preventive model. (A) Schematic diagram of subcutaneous tumors inoculation (Renca, RM-1, MC38 or Hepa1-6) after immunization with Ad-Ctrl or Ad-AURKA/CDK7 vaccine (n=5 mice per group). (B, F, J and N) Average tumor volumes of each group in the Renca, RM-1, MC38, or Hepa1-6 subcutaneous tumors were measured twice a week. The tumor volume was statistically analyzed 35 days after tumor inoculation. (C, G, K and O) The tumor volume of an individual mouse in each group of Renca, RM-1, MC38, or Hepa1-6 subcutaneous tumors was plotted. (D, H, L and P) Tumor weights were measured at the end of the experiment. (E, I, M and Q) Tumor inhibition rate in the Renca, RM-1, MC38, or Hepa1-6 subcutaneous tumors was, respectively, calculated by (D, H, L and P). The two-tailed independent Student's t-test was used to analyze two-group comparisons. The data showed as means±SD. The statistical significance levels were set as *p<0.05, **p<0.01 and ****p<0.0001. Ad, adenovirus; AURKA, Aurora kinase A; CDK7, cyclin-dependent kinase 7; i.m, intramuscular; s.c, subcutaneous.

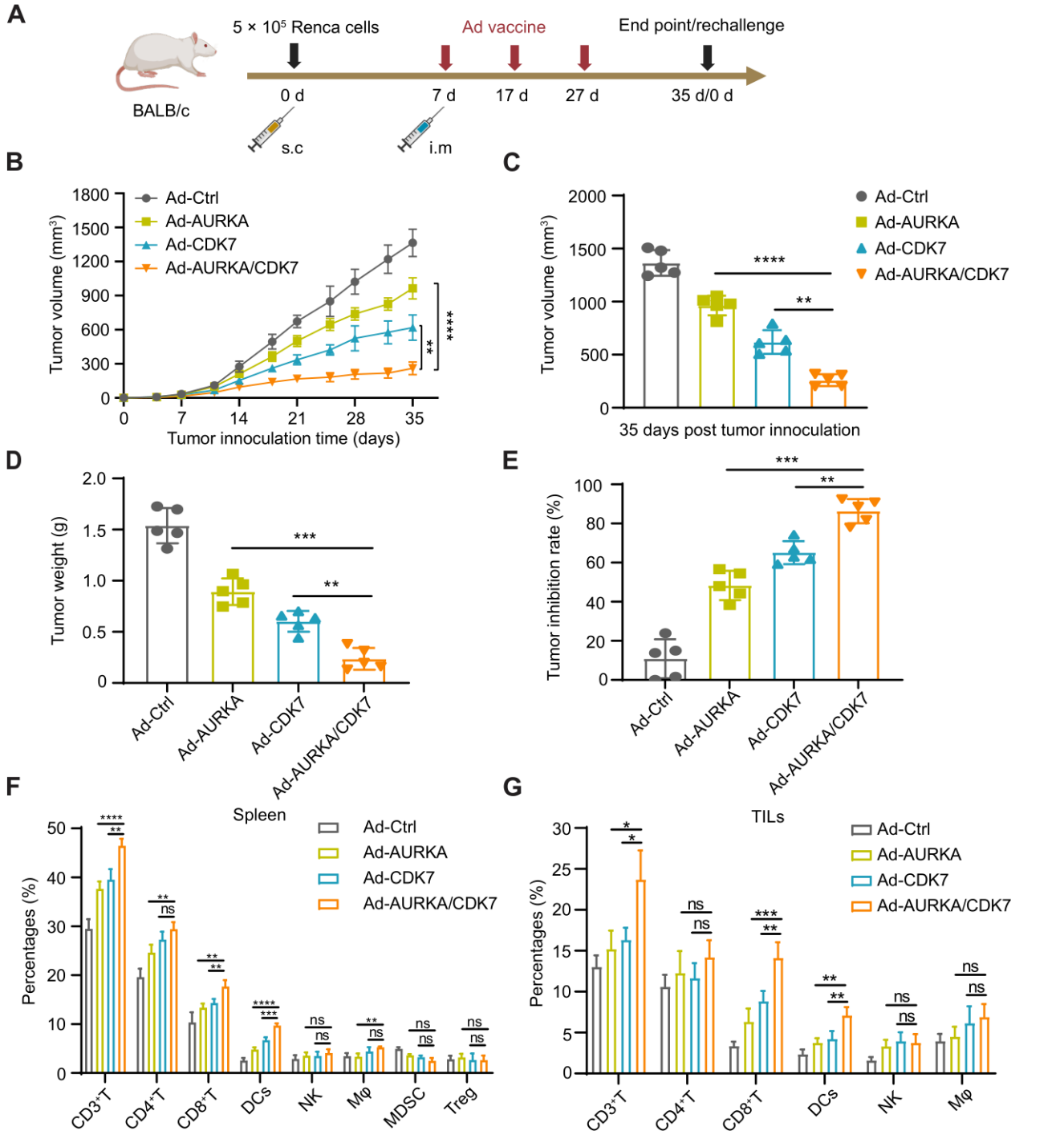

Figure 2 Antitumor efficacy of Ad-AURKA/CDK7 immunization in the Renca subcutaneous tumor model. (A) Schematic diagram showed the overall design of Renca therapeutic subcutaneous tumor (n=5 mice per group). (B) Tumor growth volume of each group after Renca tumor inoculation was measured twice a week. The tumor volume was statistically analyzed 35 days after tumor inoculation. (C) The final tumor volume of different treatment groups on day 35 after Renca tumor implantation. (D) Tumor weights were measured at the end of the experiment. (E) The tumor inhibition rate in (D) is shown. (F, G) The percentages of $CD3^+$ T cells, $CD4^+$ T cells, $CD8^+$ T cells, DCs, NK, Mϕ, MDSC, or regulatory T cells (Treg) were from spleens and tumors in each group. One-way analysis of variance was used for comparisons among multiple groups. Data are means±SD. *p<0.05, **p<0.01, ***p<0.001, ****p<0.001 and not significant (ns). Ad, adenovirus; AURKA, Aurora kinase A; CDK7, cyclin-dependent kinase 7; DCs, dendritic cells; i.m, intramuscular; MDSC, myeloid-derived suppressor cells; NK, natural killer; s.c, subcutaneous; TIL, tumor-infiltrating leukocyte.

group. The above results suggested that Ad-AURKA/CDK7 combined treatment augmented the infiltration capacity of total T cells, $CD8^+$ T cells, and DCs towards tumors, with no observed side effects on major organs.

The administration of Ad-AURKA/CDK7 vaccine promotes DCs-mediated $CD8^+$ T-cell antitumor immunity

As a crucial type of antigen-presenting cells in vivo, DCs are responsible for presenting ingested foreign antigens to T cells and initiating potent antigen-specific T-cell immune responses through Th1 cell differentiation signals.[49 50] A previous study demonstrated an increase in the maturation and proportion of $CD11c^+$ cells in the spleens after vaccination.[51] To investigate whether the Ad-AURKA/CDK7 vaccines induced this phenomenon in vivo, DC subgroups in the spleens were detected. The increased proportions of $CD11c^+$ cells and $CD8^+CD11c^+$ cells were observed in the Ad-AURKA/CDK7 group compared with the Ad-AURKA or Ad-CDK7 group (figure 3A–C). AURKA/CDK7 co-immunization raised the percentages of $CD80^+CD11c^+$, $CD86^+CD11c^+$, $MHC\text{-}II^+CD11c^+$ and $CD40^+CD11c^+$ cells (figure 3D–H). These results indicated that Ad-AURKA/CDK7 co-immunization enhanced the induction and maturation of DCs, which bolsters their phagocytosis and antigen presentation capabilities, consequently activating tumor-specific $CD8^+$ T-cell immune responses.

Similarly, as an indispensable type of functional cell responsible for killing tumors in vivo, $CD8^+$ CTLs play a pivotal role in antitumor effects and execute specific cytotoxic responses.[52] To evaluate the ability of Ad vaccines to activate $CD8^+$ T-cell immune responses, we detected the proliferation, cytokine production, and cytotoxicity of $CD8^+$ T cells in vitro. We observed higher expression levels of AURKA and CDK7 in Ad-AURKA/CDK7-infected splenocytes, DCs, and $CD8^+$ T cells compared with the control (online supplemental figure S6). Ad-AURKA/CDK7 group exhibited an increased proliferation capability of $CD8^+$ T cells (figure 4A,B). Furthermore, a similar trend was observed in the levels of IFN-γ-secreting $CD8^+$ T cells measured using the ELISpot assay in the Ad-AURKA/CDK7 treatment group (figure 4C,D). Intracellular staining results revealed that the Ad-AURKA/CDK7 vaccine resulted in a higher percentage of IFN-γ, TNF-α, and IL-2 secretion in $CD8^+$ T cells in both spleens and tumors than the Ad-AURKA or Ad-CDK7 single vaccine group (figure 4E,F). The effector cells from the co-immunization group demonstrated potent killing effects on tumor cells and displayed a superior cytolytic capability (figure 4G,H). Moreover, the proportions of central memory T cells (Tcm, $CD45^+CD8^+CD44^+CD62L^{high}$) and effector memory T cells (Tem, $CD45^+CD8^+CD44^+CD62L^{low}$) were significantly increased in the Ad-AURKA/CDK7 treated group (figure 4I,J). Concurrently, surviving mice immunized with the Ad-AURKA/CDK7 vaccine had their original tumors excised and were subsequently re-challenged with Renca tumors on the opposite side to observe the growth of the re-challenged tumors and the survival period of each group. Ad-AURKA/CDK7-treated mice exhibited the ability to inhibit the growth of the re-challenged tumors, whereas naïve mice did not (figure 4K). Moreover, Ad-AURKA/CDK7 co-immunization extended the survival time of mice after Renca tumor rechallenge (figure 4L). These results suggested that Ad-AURKA/CDK7 treatment promotes DCs-mediated $CD8^+$ T-cell antitumor immunity, and maintains a sustained antitumor effect activated by memory $CD8^+$ T cells.

Multifunctional $CD8^+$ T cells are required for the therapeutic effect of Ad-AURKA/CDK7 vaccine

To trigger a powerful antitumor response, multifunctional $CD8^+$ T cells played an important role in inducing necrosis and apoptosis of tumor cells and producing various cytokines such as IFN-γ, TNF-α, and IL-2.[51] Subsequently, we compared the percentages of antigen-specific $CD8^+$ T cells in each group that secreted two or more cytokines in splenic immune cells and tumor-infiltrating $CD8^+$ T cells. As expected, the proportions of $CD8^+$ T cells secreting $TNF\text{-}\alpha^+IFN\text{-}\gamma^+$, $TNF\text{-}\alpha^+IL\text{-}2^+$, $IFN\text{-}\gamma^+IL\text{-}2^+$, and $TNF\text{-}\alpha^+IFN\text{-}\gamma^+IL\text{-}2^+$ in the spleens of the Ad-AURKA/CDK7 group were higher than those in the spleens of the Ad-AURKA or Ad-CDK7 group (figure 5A–D). A similar trend was observed in tumor-infiltrating $CD8^+$ T cells in subcutaneous tumors of the Ad-AURKA/CDK7 combined group (figure 5E–H). These results suggested that multifunctional $CD8^+$ T cells producing various cytokines in combination immunization significantly strengthen tumor-suppressive effects. Additionally, to elucidate whether $CD8^+$ T cells were decisive for antitumor immune responses in the Ad-AURKA/CDK7 vaccines, we used an anti-CD8 mAb to deplete tumor-specific $CD8^+$ T cells in vivo. The $CD8^+$ T-cell depletion assay indicated that the antitumor effects of the combination vaccine disappeared. The weights of subcutaneous tumors were significantly increased, and tumor inhibition rates were reduced after $CD8^+$ T-cell depletion (figure 5I,J). Furthermore, the percentages of $CD8^+$ T cells and $CD8^+CD11c^+$ DCs were significantly decreased in the spleens and tumors of the anti-CD8 mAb-treated group (figure 5K,L). The above results indicated that antigen-specific multifunctional $CD8^+$ T cells play a decisive role in the antitumor immune responses induced by the Ad-AURKA/CDK7 vaccine.

Ad-AURKA/CDK7 treatment inhibits tumor growth and metastasis in the lung metastasis and orthotopic models by enhancing $CD8^+$ T-cell immune responses

A previous study reported that the lung is a common site of renal carcinoma metastasis.[53] For the lung metastasis model, mice were intramuscularly immunized with various Ad vaccines on days 1, 8, and 15 (figure 6A). To explore the antitumor activity of the combined vaccine, some mice were sacrificed and their lungs were excised on day 28 post tumor inoculation. The number of tumor metastatic nodules on the lung surface was significantly reduced in the combined treatment group compared with

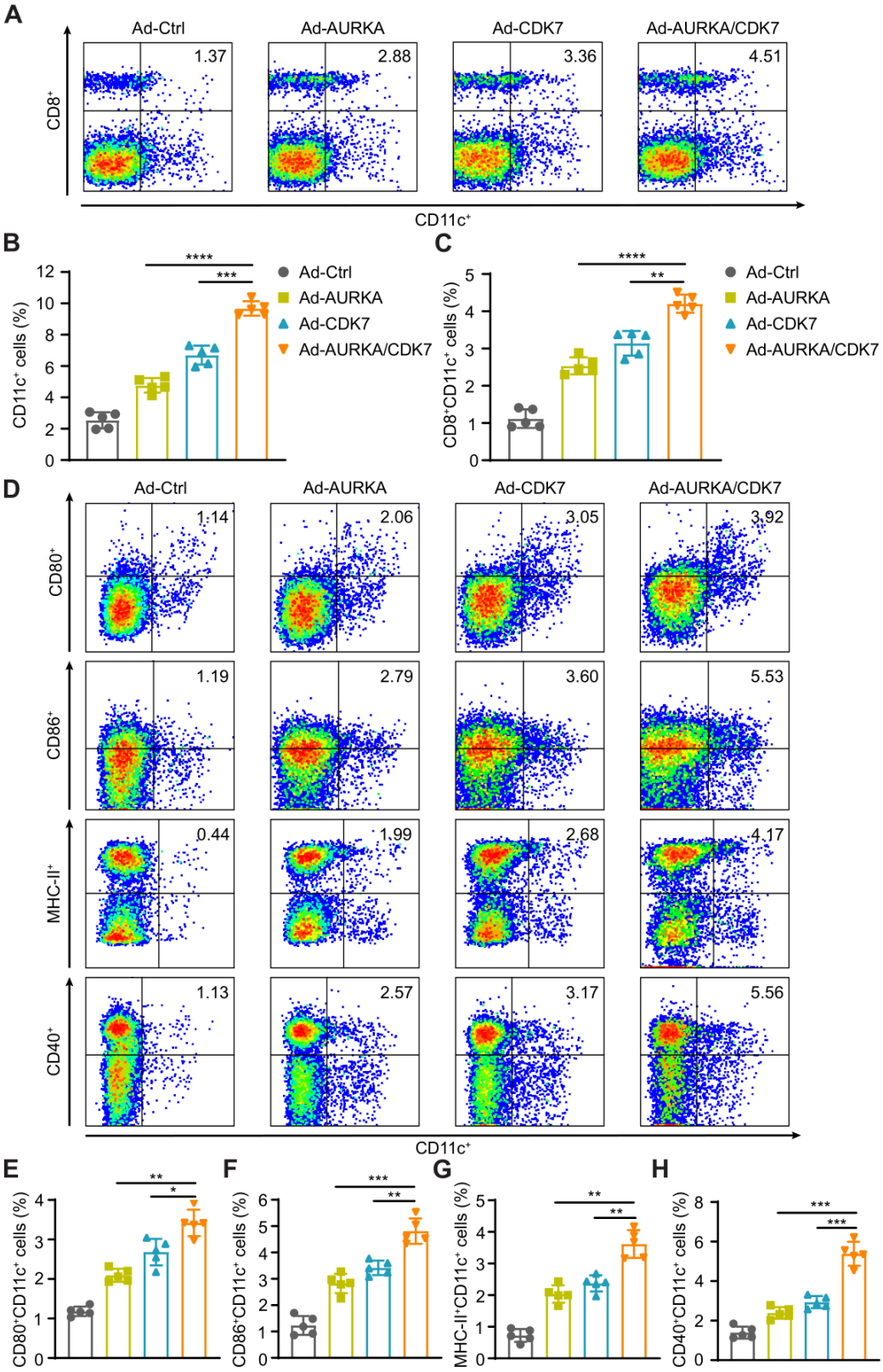

Figure 3 The maturation and differentiation of DC subgroups induced by Ad-AURKA/CDK7 vaccine in vivo. Different DC subgroups in spleens were analyzed by flow cytometry at the end of the experiments. (A) The percentages of $CD8^+CD11c^+$ DC subsets in immunized mice of each group (n=5), a typical flow cytometry data is displayed from each group. (B, C) Statistical analysis of the ratio of $CD11c^+$ DCs or $CD8^+CD11c^+$ DCs. (D) The representative flow cytometry data of the percentage of $CD80^+CD11c^+$, $CD86^+CD11c^+$, MHC-II^+CD11c^+, or $CD40^+CD11c^+$ DC subsets in spleens of each group. (E–H) Statistical analysis of different DC subgroups in (D). One-way analysis of variance was used for comparisons among multiple groups. Data are means±SD. *p<0.05, **p<0.01, ***p<0.001 and ****p<0.001. Ad, adenovirus; AURKA, Aurora kinase A; CDK7, cyclin-dependent kinase 7; DCs, dendritic cells.

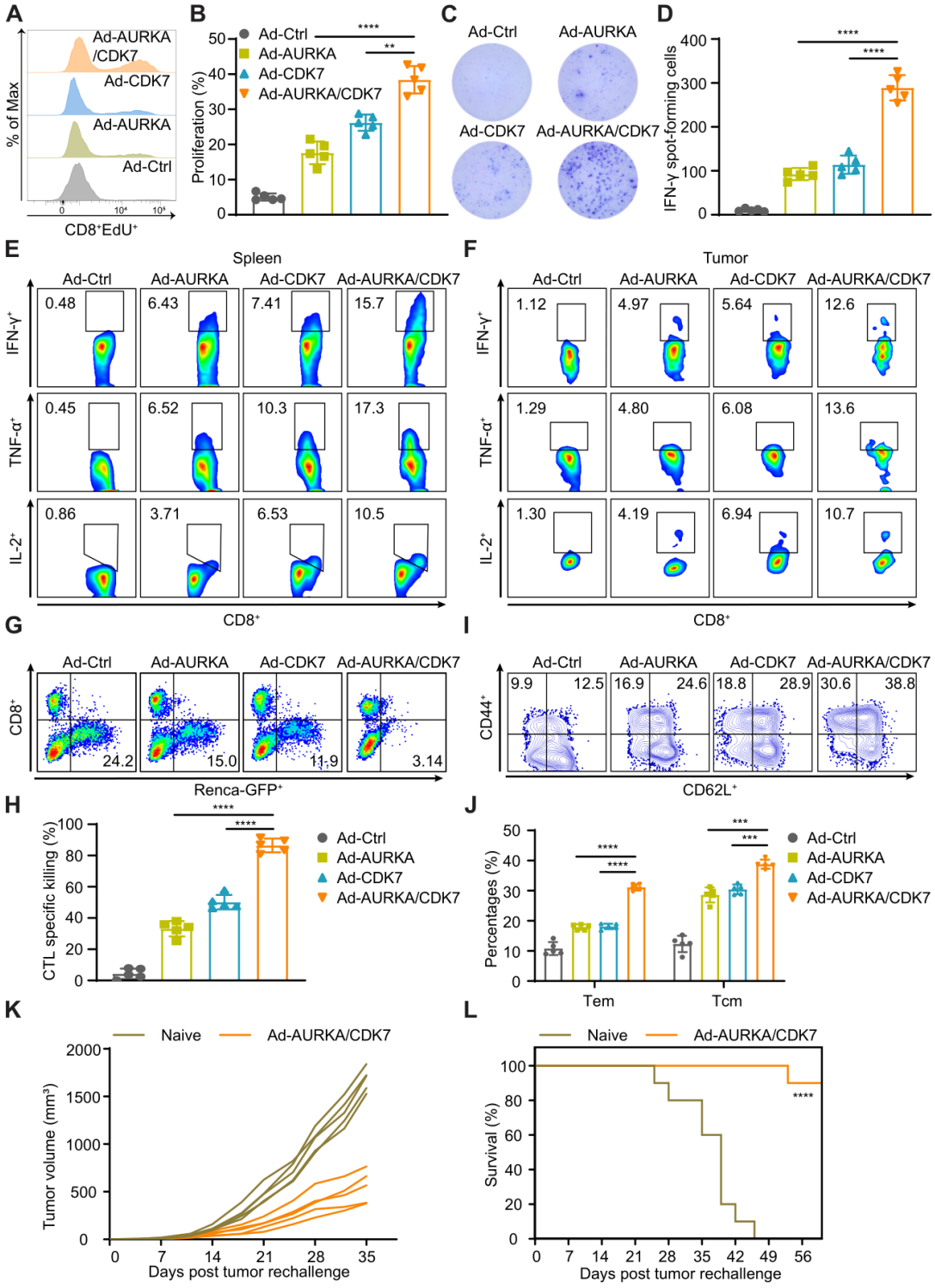

Figure 4 Ad-AURKA/CDK7 treatment induced memory CD8⁺ T-cell immune response. (A, B) The proliferation capability of antigen-specific CD8⁺ T cells from mice spleens in each group was detected by the EdU assay after the continuous stimulation with AURKA/CDK7 antigens. (C, D) The number of IFN-γ-secreting T lymphocytes was observed using the ELISpot assay. (E, F) The representative flow cytometry data of CD8⁺ T cells secreting IFN-γ, TNF-α, or IL-2 in each group after antigen stimulation. (G, H) The co-culture experiment was detected to assess CTL-specific killing ability. (I, J) The proportions of effector memory T cells or central memory T cells in spleens were measured, and typical flow cytometry data was selected from each group. (K) The tumor volume of a single mouse in the Renca subcutaneous tumors was measured twice a week after tumor rechallenge (n=5 mice per group). (L) The survival curve of the Ad-AURKA/CDK7 or Ad-Ctrl group was observed after re-implantation of the Renca tumor (n=10 mice per group). One-way analysis of variance was used for comparisons among multiple groups. Survival analysis was performed using the log-rank (Mantel-Cox) test. Data are means±SD. **p<0.01, ***p<0.001, ***p<0.001 and ****p<0.0001. Ad, adenovirus; AURKA, Aurora kinase A; CDK7, cyclin-dependent kinase 7; CTL, cytotoxic T lymphocytes; ELISpot, enzyme-linked immunosorbent spot; IFN, interferon; IL, interleukin; TNF, tumor necrosis factor.

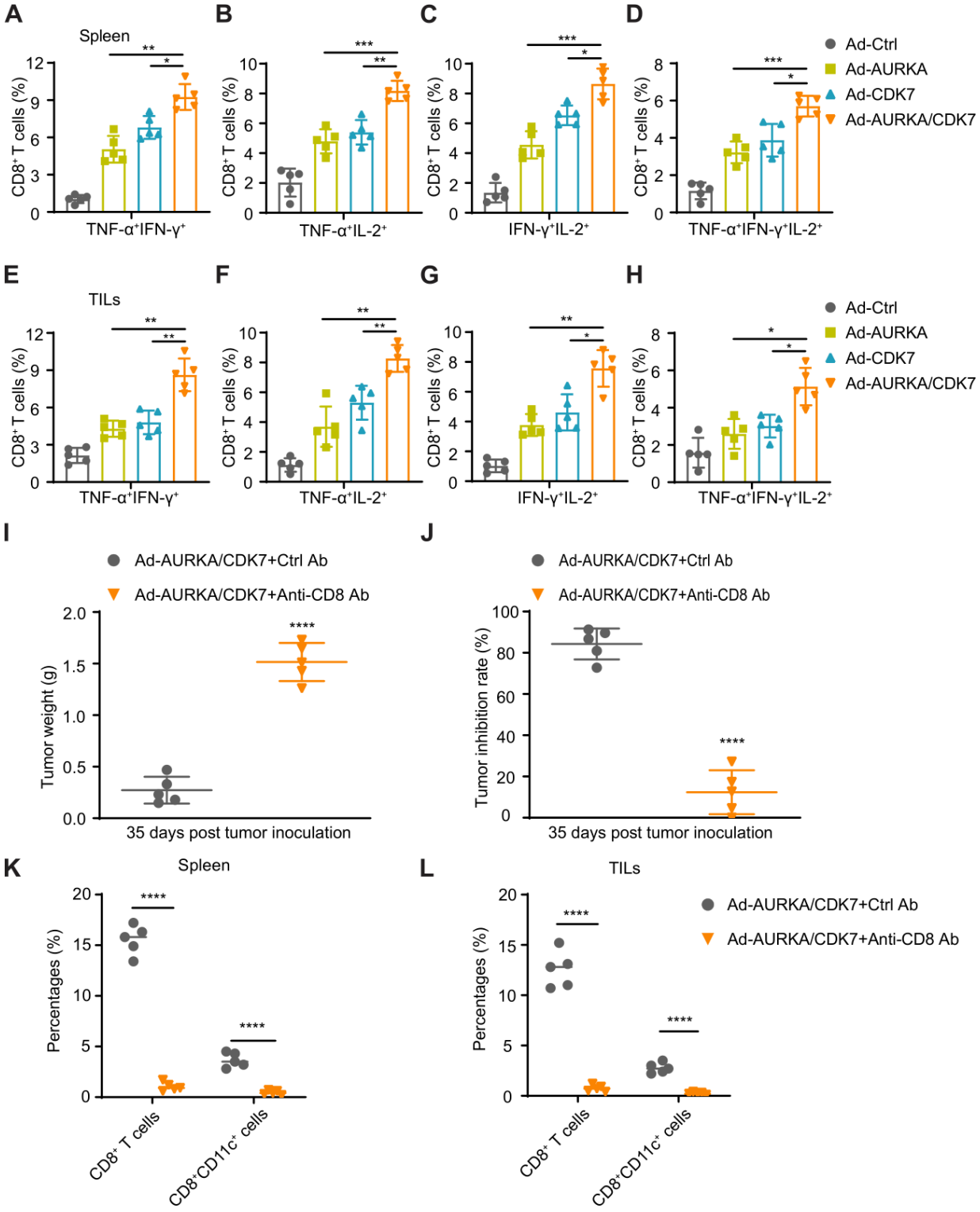

Figure 5 Multifunctional CD8$^+$ T cells exerted an indispensable role in the antitumor effects of Ad-AURKA/CDK7 vaccine. (A–D) The percentages of multifunctional CD8$^+$ T cells secreting TNF-α$^+$IFN-γ$^+$, TNF-α$^+$IL-2$^+$, IFN-γ$^+$IL-2$^+$, or TNF-α$^+$IFN-γ$^+$IL-2$^+$ in spleens of each group were detected by flow cytometry after continuous stimulation with AURKA/CDK7 antigens for 96 hours. (E–H) The proportions of tumor-infiltrating multifunctional CD8$^+$ T lymphocytes secreting TNF-α$^+$IFN-γ$^+$, TNF-α$^+$IL-2$^+$, IFN-γ$^+$IL-2$^+$ or TNF-α$^+$IFN-γ$^+$IL-2$^+$ in tumor tissues of each group were analyzed on day 35 after Renca tumor inoculation. (I) The tumor weights of mice in each group were measured at the end of CD8 depletion. (J) Tumor inhibition rates in (I). (K, L) The percentages of CD8$^+$ T cells or CD8$^+$CD11c$^+$ DCs were detected in spleens and tumor tissues of each group in the CD8$^+$ T-cell depletion assay. The two-tailed independent Student's t-test was used to analyze two-group comparisons. One-way analysis of variance was used for comparisons among multiple groups. The data are shown as means±SD, with n=5 mice per group. *p<0.05, **p<0.01, ***p<0.001 and ****p<0.0001. Ad, adenovirus; AURKA, Aurora kinase A; CDK7, cyclin-dependent kinase 7; IFN, interferon; IL, interleukin; TIL, tumor-infiltrating leukocytes; TNF, tumor necrosis factor.

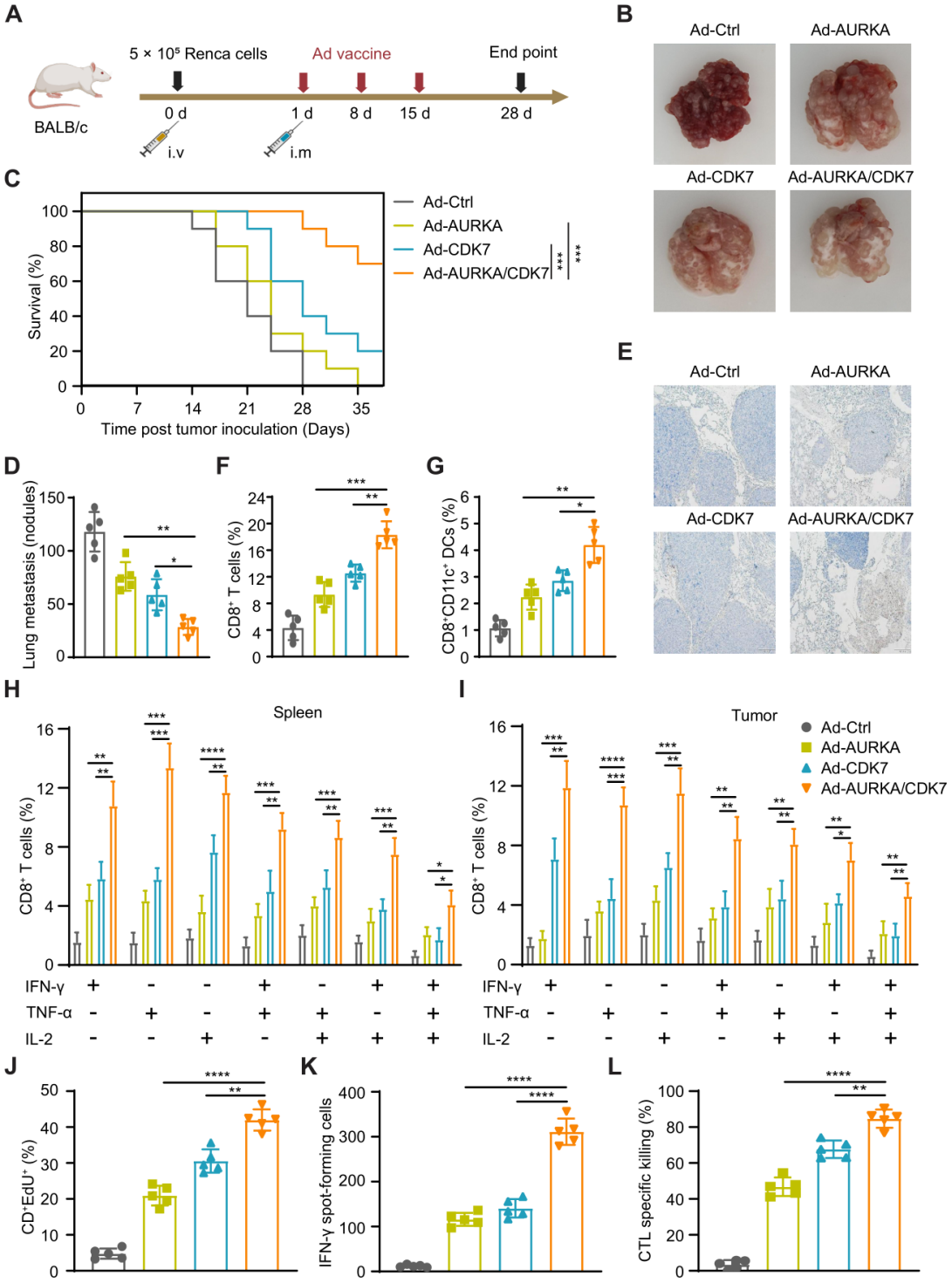

Figure 6 Ad-AURKA/CDK7 treatment suppressed tumor metastases by activating multifunctional CD8⁺ T cells. (A) A schematic diagram displayed the design and treatment of lung metastasis. (B) The representative image of lung metastasis nodules in each group. (C) The survival curve of mice in different groups after Renca tumor lung metastasis (n=10 mice per group). (D) The number of metastatic nodules was counted on the lung surface of immunized mice (n=5 mice per group). (E) Typical immunohistochemistry image of the lung-infiltrating CD8⁺ T cells in each group immunized with different vaccines. The scale was 200 µm. (F, G) The proportion of CD8⁺ T cells and CD8⁺CD11c⁺ DCs in the lungs of treated mice in each group. (H, I) Percentages of multifunctional CD8⁺ T lymphocytes producing IFN-γ, TNF-α, or IL-2 in spleens and tumor tissues of different groups. (J) The EdU assay was used to detect the proliferation of CD8⁺ T cells. (K) The number of IFN-γ-secreting T lymphocytes was counted using ELISpot assay. (L) The percentages of tumor-specific killing capability of CTL in each group. One-way analysis of variance was used for comparisons among multiple groups. Survival analysis was performed using the log-rank (Mantel-Cox) test. The data expressed as means±SD. *p<0.05, **p<0.01, ***p<0.001, and ****p<0.0001. Ad, adenovirus; AURKA, Aurora kinase A; CDK7, cyclin-dependent kinase 7; CTL, cytotoxic T lymphocyte; DC, dendritic cell; ELISpot, enzyme-linked immunosorbent spot; IFN, interferon; IL, interleukin; i.m, intramuscular; i.v, intravenous; TNF, tumor necrosis factor.

the other treatment groups (figure 6B,D), Ad-AURKA/CDK7 co-immunization effectively prolonged the survival of mice (figure 6C). Furthermore, IHC and flow cytometry results indicated that the ratios of tumor-infiltrating $CD8^+$ T cells in the Ad-AURKA/CDK7 group were higher than those in the other groups (figure 6E,F). In addition, a similar trend of $CD8^+CD11c^+$ DCs was observed in the combined immunization group (figure 6G). Notably, the percentages of multifunctional $CD8^+$ T cells in the spleens and tumors were significantly increased in the Ad-AURKA/CDK7 group (figure 6H,I). Moreover, the proliferation assay of $CD8^+$ T cells suggested that Ad-AURKA/CDK7 co-immunization enhanced the proliferation ability of antigen-specific $CD8^+$ T cells (figure 6J). A significant increase in IFN-γ^+ secreted by T cells was also shown in the Ad-AURKA/CDK7 group (figure 6K). Likewise, the co-culture experiment indicated that $CD8^+$ T cells from the combined treatment effectively killed Renca cells (figure 6L).

Similarly, to establish the orthotopic model, 1×10^5 Renca cells were implanted into the left kidney of each mouse. After tumor cell inoculation, the mice were intramuscularly immunized with different vaccines three times (figure 7A). As anticipated, Ad-AURKA/CDK7 combined immunization suppressed tumor progression compared with that in the single-vaccine group (figure 7B). Meanwhile, co-immunization with Ad-AURKA/CDK7 prolonged the survival period of tumor-bearing mice (figure 7C). Tumor weights were reduced, and the tumor inhibition rate was increased (figure 7D,E). These results directly revealed the effectiveness of the combined vaccine. Furthermore, immunohistochemistry of orthotopic kidney tumors also showed that tumor-infiltrating $CD8^+$ T cells in the co-immunization treatment group were higher than those in the other treatment groups (figure 7F). Additionally, the proportions of $CD8^+$ T cells and $CD8^+CD11c^+$ DCs in the Ad-AURKA/CDK7 group were significantly increased (figure 7G,H). The results of tumor-infiltrating multifunctional $CD8^+$ T cells suggested that the percentages of TNF-α^+IL-2^+, TNF-α^+IFN-γ^+ $CD8^+$, IFN-γ^+IL-2^+ $CD8^+$, and TNF-α^+IFN-γ^+IL-2^+ $CD8^+$ T cells in the combined group's spleens and tumors were dramatically increased (figure 7I,J). The proliferation assay showed that $CD8^+$ T cells had higher proliferative abilities in the co-immunization group (figure 7K). An increased proportion of CTL-specific killing was also observed in the Ad-AURKA/CDK7 group (figure 7L). Taken together, these results indicated that Ad-AURKA/CDK7 combination treatment exerted a significant inhibitory effect on the advancement of lung metastasis and orthotopic kidney tumors by multifunctional $CD8^+$ T-cell antitumor immune responses.

Ad-hAURKA/CDK7 exhibits a potent therapeutic efficacy in the tumor model of humanized mice

Ad-AURKA/CDK7 vaccine facilitated the induction and maturation of DCs, and increased the proportion of multifunctional $CD8^+$ T cells, resulting in the inhibition of tumor growth across subcutaneous, lung metastasis, and orthotopic models. To align with the actual clinical applicability, we reconstructed the human Ad-AURKA vaccine (Ad-hAURKA), while the Ad-CDK7 vaccine was administered repeatedly because of its homology with humans and mice. Using the original subcutaneous planting model, OSRC-2 renal cancer cells were subcutaneously implanted into humanized mice on day 0, followed by immunization with Ad-hAURKA/CDK7 or Ad-Ctrl on days 7, 17, and 27 (figure 8A). Ad-hAURKA/CDK7 treatment decreased the final tumor volumes and weights (figure 8B,C) and elevated the tumor inhibition rate (figure 8D). To elucidate the mechanism of tumor suppression, immune cells in the spleen and tumor tissues were analyzed. There was a significant increase in the percentages of DC subgroups in the spleens, such as $CD8^+CD11c^+$, $CD103^+CD11c^+$, $CD80^+CD11c^+$, $CD86^+CD11c^+$ and $HLA\text{-}A2^+CD11c^+$ (figure 8E–J). Similarly, the proportions of DCs in tumor tissues, including $CD8^+CD11c^+$, $CD103^+CD11c^+$, $CD80^+CD11c^+$, $CD86^+CD11c^+$, and $HLA\text{-}DR^+CD11c^+$, showed effective improvement (figure 8K–O). These findings indicated the induction and maturation of more DC subgroups following Ad-hAURKA/CDK7 treatment. The analysis of IFN-γ, TNF-α, and IL-2 on multifunctional $CD8^+$ T cells revealed that the Ad-hAURKA/CDK7 vaccine activated multifunctional $CD8^+$ T cells to produce more cytokines in spleen and tumor tissues (figure 8P–R). Additionally, the ratio of multifunctional $CD8^+$ T cells secreting two or more cytokines in the combined group was significantly increased (figure 8S,T). In summary, these results showed that the Ad-hAURKA/CDK7 vaccine effectively inhibited tumor growth by modulating DC subgroups and multifunctional $CD8^+$ T cells in humanized mice, consistent with the conclusions of previous experiments in wild-type mice.

DISCUSSION

Cancer vaccines, considered a promising therapeutic strategy in the immunotherapy of solid tumors, have the potential to alleviate immune suppression within tumors and elicit cellular and humoral immunity against tumor antigens.[54] Therapeutic cancer vaccines aim to establish persistent antitumor immune memory and induce tumor regression.[55] Ad, an ideal vector for delivering target genes to immune cells in vivo, exerts a potent adjuvant effect due to its intrinsic stimulation.[56] Moreover, replication-defective Ad vectors improved persistent immunogenicity and ensured its safety.[57 58] In this study, we developed a cancer vaccine that efficiently encoded AURKA or CDK7 using a replication-deficient Ad. To evaluate the antitumor efficacy of combination immunization, five tumor models were established, including prophylactic, subcutaneous, lung metastasis, orthotopic, and humanized mice tumor models. The design rationale behind these tumor models is to simulate the immune evasion, recurrence, and metastasis characteristics of solid tumors. Tumor

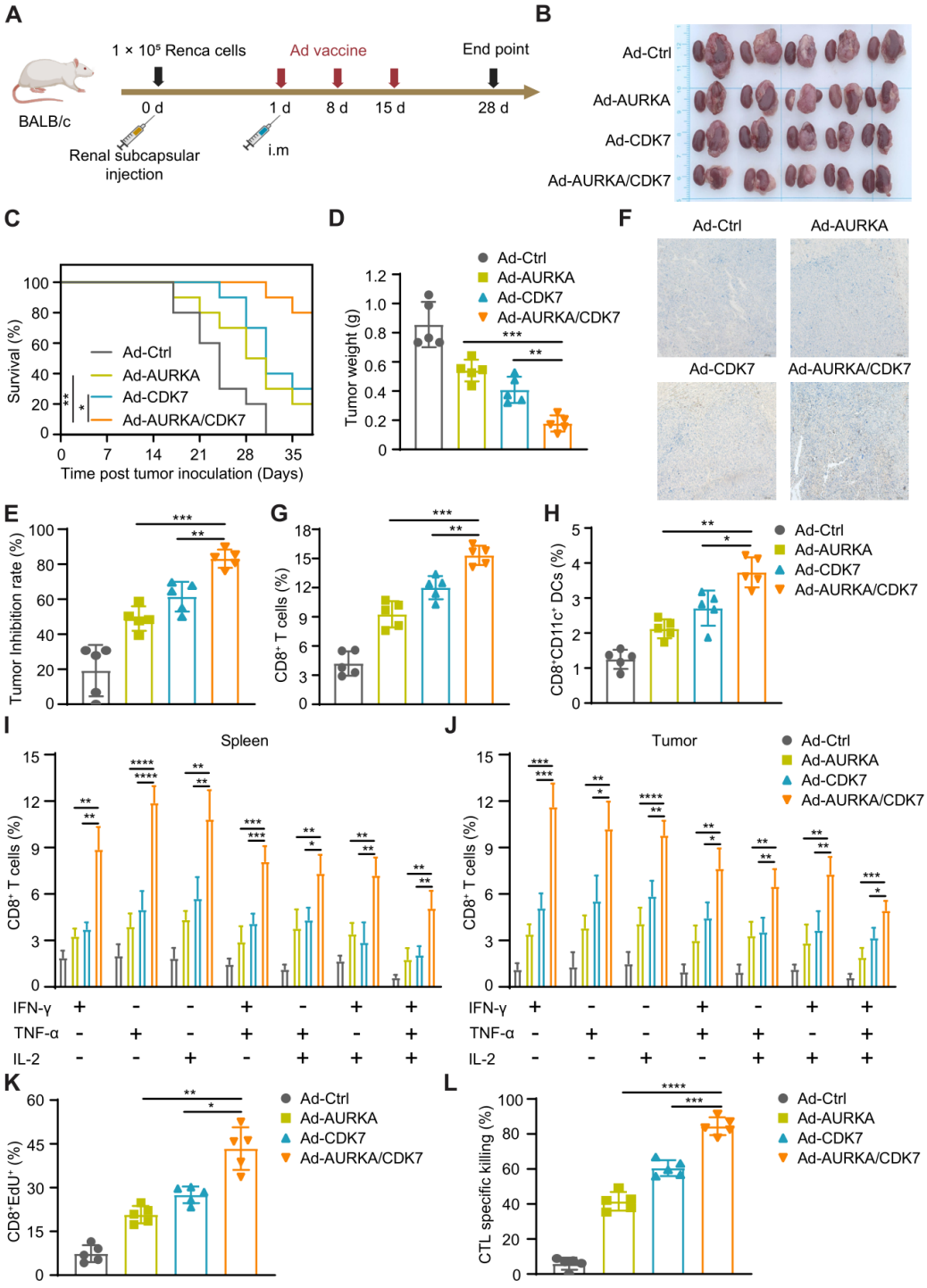

Figure 7 Antitumor efficacy of Ad-AURKA/CDK7 vaccine requires for multi-functional CD8⁺ T cells in the Renca orthotopic model. (A) Schematic diagram illustrating the design of the Renca orthotopic model and vaccination. (B) Typical image of renal orthotopic tumors in the different vaccine-treated groups at the endpoint of the experiment (n=5 mice per group). (C) The survival curve of each group in the orthotopic model (n=10 mice per group). (D) Tumor weights were calculated by the formula: Tumor mass (g)=left kidney mass – right kidney mass. (E) Tumor inhibition rate in (D). (F) Tumor-infiltrating CD8⁺ T lymphocytes were captured by immunohistochemical staining in the left kidney and the representative images were shown. The scale was 200 µm. (G, H) Statistical analysis of the proportion of CD8⁺ T cells or CD8⁺CD11c⁺ DCs in renal tumor tissues of each group. (I, J) The percentages of multifunctional CD8⁺ T lymphocytes secreting IFN-γ⁺, TNF-α⁺, IL-2⁺, TNF-α⁺IFN-γ⁺, TNF-α⁺IL-2⁺, IFN-γ⁺IL-2⁺, or TNF-α⁺IFN-γ⁺IL-2⁺ were detected by flow cytometry in spleens and tumors in each group. (K) The antigen-stimulated proliferation of CD8⁺ T cells in different groups. (L) The tumor-specific killing capability of CTL was detected by the co-culture experiment. One-way analysis of variance was used for comparisons among multiple groups. Survival analysis was performed using the log-rank (Mantel-Cox) test. The data are shown as means±SD. *p<0.05, **p<0.01, ***p<0.001, and ****p<0.0001. Ad, adenovirus; AURKA, Aurora kinase A; CDK7, cyclin-dependent kinase 7; CTL, cytotoxic T lymphocyte; DC, dendritic cell; IFN, interferon; IL, interleukin; i.m, intramuscular; s.c, subcutaneous; TNF, tumor necrosis factor.

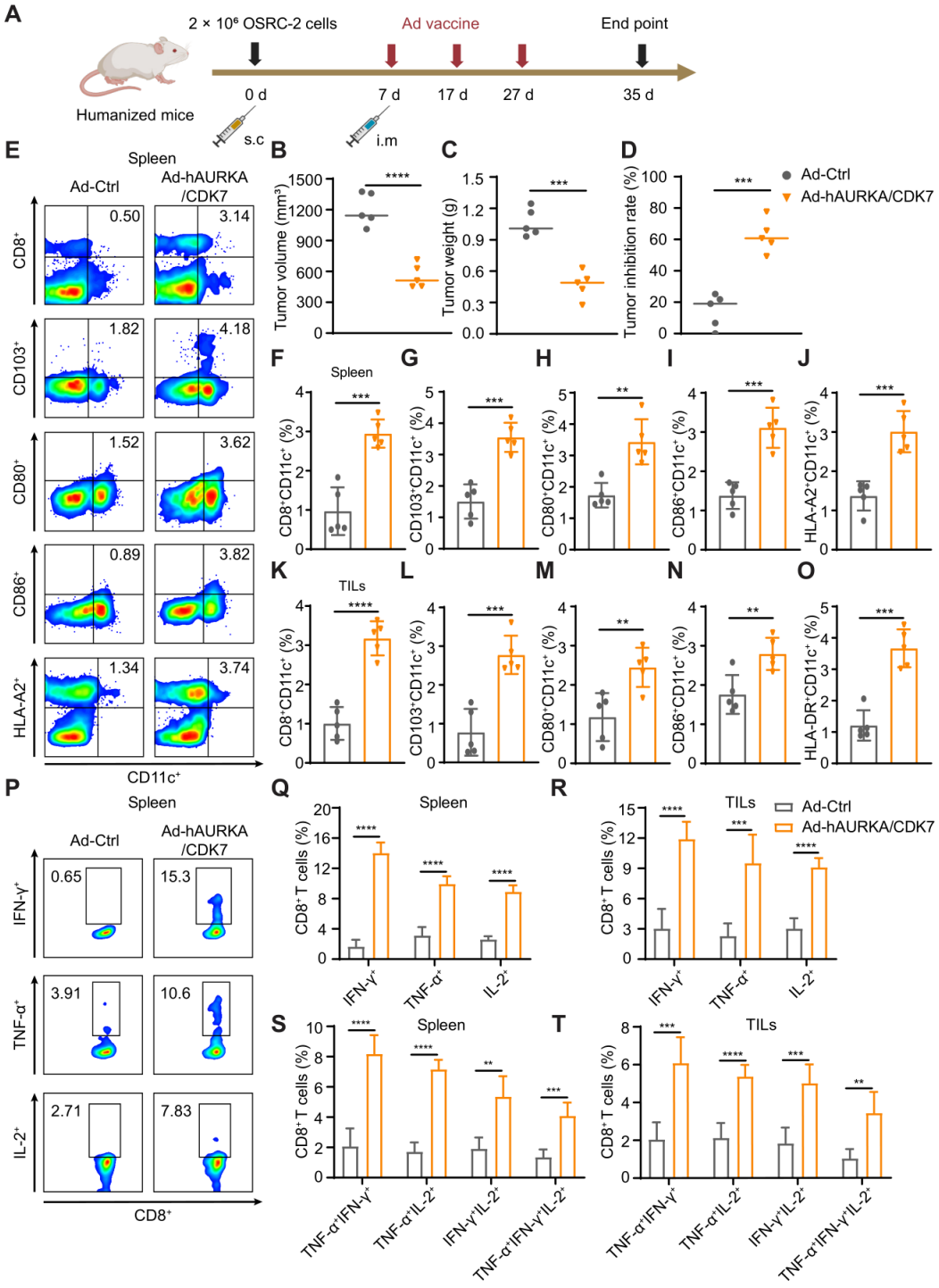

Figure 8 The therapeutic effect induced by Ad-AURKA/CDK7 vaccine in the humanized mice model. (A) Schematic diagram explaining the establishment of the humanized mice model and experiment design. (B) Final tumor volumes were measured in each group on day 35 after OSRC-2 tumor inoculation. (C) Tumor weights of each group at the end of the experiment. (D) Tumor inhibition rate in (C). (E) The representative flow cytometry data of $CD8^+CD11c^+$, $CD103^+CD11c^+$, $CD80^+CD11c^+$, $CD86^+CD11c^+$, and $HLA\text{-}A2^+CD11c^+$ DC subgroups in spleens of each group. (F–J) Statistical analysis of DC subsets in (E) in the spleens of humanized mice. (K–O) The proportions of tumor-infiltrating DC subsets in different groups were detected. (P) The typical flow cytometry image of multi-functional $CD8^+$ T lymphocytes secreting IFN-γ^+, TNF-α^+, or IL-2^+ in spleens in the Ad-Ctrl or Ad-hAURKA/CDK7 treatment group. (Q, S) The percentages of multifunctional $CD8^+$ T cells in (P) in spleens. (R, T) Statistical analysis of the proportion of IFN-γ^+CD8^+, TNF-α^+CD8^+, IL-2^+CD8^+, TNF-α^+IFN-γ^+CD8^+, TNF-α^+IL-2^+CD8^+, IFN-γ^+IL-2^+CD8^+, or TNF-α^+IFN-γ^+IL-2^+CD8^+ in antigen-specific $CD8^+$ T lymphocytes of tumor tissues per group. The two-tailed independent Student's t-test was used to analyze two-group comparisons. One-way analysis of variance was used for comparisons among multiple groups. The data are shown as means±SD, with n=5 mice per group. **p<0.01, ***p<0.001, and ****p<0.0001. Ad, adenovirus; AURKA, Aurora kinase A; CDK7, cyclin-dependent kinase 7; DC, dendritic cell; IFN, interferon; IL, interleukin; i.m, intramuscular; TIL, tumor-infiltrating leukocytes; TNF, tumor necrosis factor..

volumes and weights served as indicators to assess the effectiveness of the Ad-AURKA/CDK7 vaccine. Examination of the normal structure of the heart, liver, lung, and kidney revealed no apparent cytotoxicity or serious side effects associated with Ad vaccines.

Proper antigen selection can double the effectiveness of cancer vaccine treatment with half the effort. Traditional vaccine targets have a limited range of action and may not induce a strong immune response. However, the kinase family is consistently highly expressed in tumors and controls tumor proliferation and division, making them favorable targets for tumor antigens. As a family of serine/threonine kinases, AURKA is highly expressed in various tumors, including renal cell carcinoma, prostate cancer, colorectal cancer, and liver cancer, establishing it as one of the most promising therapeutic targets.[44 45 59] Similarly, CDK7, a member of the serine/threonine kinases family, regulates cell proliferation, division, and tumor growth by influencing cell cycle transition and transcription.[35 60] Moreover, the expression of CDK7 is significantly elevated in renal cell carcinoma, prostate cancer, and colorectal cancer compared with that in normal tissues.[39 46 48] Therefore, for the preventive experiment, we selected Renca cells (renal cell carcinoma), RM-1 (prostate cancer), MC38 (colorectal cancer), and Hepa1-6 (liver cancer) as our tumor models. Simultaneously, Ad-AURKA and Ad-CDK7 were constructed under the binding of Ad with robust immunogenicity, and their high expression was confirmed. As anticipated, all four tumor types were effectively suppressed by Ad-AURKA/CDK7 treatment in the preventive model. This observed phenomenon was consistent with the characteristics of the kinase family, indicating that delivering kinase targets through an Ad vaccine presented a novel approach for solid tumor immunotherapy.

In the prophylactic model, Renca tumor cells were chosen from the aforementioned tumors due to their high tumor inhibition rate. A similar trend of tumor suppression was observed in subcutaneous, lung metastasis, orthotopic, and humanized mice tumor models. To unravel the underlying mechanism behind the strong antitumor immune response induced by the Ad-AURKA/CDK7 vaccine, we examined tumor tissues and spleens of vaccine-immunized mice. As expected, Ad-AURKA/CDK7 treatment increased the proportion of $CD11c^+$ DCs and promoted their induction and maturation, including $CD8^+CD11c^+$, $CD80^+CD11c^+$, $CD86^+CD11c^+$, $MHC\text{-}II^+CD11c^+$ and $CD40^+CD11c^+$ DCs. These mature DCs played a role in directly presenting tumor-specific antigens to $CD8^+$ T cells and activating cytotoxic T lymphocyte responses, while also indirectly inducing the activation of $CD4^+$ T cells and B cells. Previous research suggested that $CD4^+$ T cells and antibodies produced by activated B cells assisted antigen-specific $CD8^+$ T cells in inducing a robust antitumor immune response.[61–63] Following stimulation with specific antigens, the proliferation of $CD8^+$ T cells in Ad-AURKA/CDK7 co-immunization was significantly enhanced. Simultaneously, a notable increase was observed in the percentages of Tcm and Tem in the Ad-AURKA/CDK7 group, and there was an improved production of cytokines by multifunctional $CD8^+$ T cells in both tumors and spleens. Antigen-stimulated $CD8^+$ T cells demonstrated a strong capability to kill tumor cells and induce an antitumor immune response. This comprehensive analysis further elucidated the mechanism by which Ad-AURKA/CDK7 combined vaccines activated antitumor immunity and suppressed tumor growth.

Recognized as the primary executor of the antitumor immune response, $CD8^+$ T cells played a crucial role in the secretion of various cytokines. We observed an increase in the proportions of $TNF\text{-}\alpha^+IL\text{-}2^+$, $TNF\text{-}\alpha^+IFN\text{-}\gamma^+$, $IFN\text{-}\gamma^+IL\text{-}2^+$, and $TNF\text{-}\alpha^+IFN\text{-}\gamma^+IL\text{-}2^+$ $CD8^+$ T cells in the AURKA/CDK7 treatment group, signifying that multifunctional T cells directly eliminated tumor cells. Following a 48-hour co-culture of $CD8^+$ T cells and Renca cells, the residual proportion of tumor cells indicated that the Ad-AURKA/CDK7 vaccine effectively controlled tumor growth by modulating the antitumor immune response of $CD8^+$ T cells. To further confirm this, mAb was employed to deplete $CD8^+$ T cells in vivo. As a result, the Ad-AURKA/CDK7 no longer suppressed tumor growth, confirming our hypothesis that the vaccine activated $CD8^+$ T-cell immune responses against tumor progression. A previous study noted that cancer vaccines could trigger the dual activation of cellular and humoral immunity.[64] In cellular immunity, with the support of the Ad's strong immunogenicity and "self-adjuvants", our Ad-AURKA/CDK7 vaccines initially increased the induction and maturation of DCs. Subsequently, mature DCs presented tumor-specific antigens to $CD8^+$ T cells, activating $CD8^+$ T cells to initiate a tumor-specific immune response. In this study, an effective exploration of humoral immunity has not yet been conducted. Undoubtedly, the vaccine-induced AURKA or CDK7 antibodies also play an essential role in helping and stimulating antigen-specific $CD8^+$ T cells. AURKA or CDK7 specific antibody can also block both AURKA or CDK7 positive tumor cells to induce tumor cell apoptosis and further activate DCs-mediated $CD8^+$ T-cell immune response. Therefore, we will further investigate the efficacy of vaccine-induced antibodies in tumor suppression in further experiments.

The therapeutic efficacy of the Ad-AURKA/CDK7 vaccine was observed in the subcutaneous model. However, renal carcinoma exhibited a higher propensity for orthotopic implantation and lung metastasis. Consequently, we investigated immunoreaction and tumor-suppressive effects in lung metastatic and orthotopic models. A similar tendency was observed, indicating that Ad-AURKA/CDK7 combined vaccines not only effectively reduced the tumor burden, but also activated the antitumor function of $CD8^+$ T cells. Moreover, co-immunization extended the survival period of the mice. This can be reasonably attributed to the increased infiltration of $CD8^+$ T cells into tumor tissue, which induced an immune response for the removal of tumor cells. Cytokines

secreted by $CD8^+$ T cells also played a crucial role in the antitumor efficacy. Additionally, to address practical clinical challenges, we validated the antitumor effects of the combination vaccine in humanized mice. Similarly, co-immunization significantly enhanced the proportion of $CD11c^+$ DC subsets and multifunctional $CD8^+$ T cells in the spleens and tumors, with increased cytokine secretion by multifunctional $CD8^+$ T cells against tumor growth. Therefore, the observed phenomenon in humanized mice also indicated that Ad-hAURKA/CDK7 robustly triggered an immune response mechanism to counteract tumor progression. Unfortunately, some tumors persisted at the end of the experiment. Several factors may have contributed to this outcome. Immune tolerance may develop after three instances of the same Ad immunization. Antibodies against Ad proteins can be produced in the body. To enhance therapeutic efficacy and immunogenicity in clinical research, alternative delivery carriers and administration methods, such as intertumoral and mucosal administration, should be considered. we will consider reducing the number of repeated immunizations or combining our Ad vaccine with wild-type vectors or other Ad vector-mediated vaccines (such as Ad5/F35, Ad26, or ChAdOx1) as a boost in future clinical applications. It is important to note that this study primarily aimed to demonstrate the use of kinases as vaccines for treating solid tumors. The aforementioned administration methods will require continuous optimization in subsequent experiments.

In conclusion, our experimental data confirmed that the Ad-AURKA/Ad-CDK7 vaccine induced DCs maturation, activated DC-mediated $CD8^+$ T-cell immune responses, and enhanced cytokine secretion in multifunctional T cells. This co-immunization effectively suppressed the progression of solid tumors in both the wild-type and humanized mice. Consequently, AURKA and CDK7 have emerged as ideal targets against solid tumor growth. The Ad-AURKA/CDK7 vaccine presents a novel and promising therapeutic strategy for the prognosis of solid tumors.

Author affiliations
[1]Cancer Institute, Xuzhou Medical University, Xuzhou, Jiangsu, China
[2]Center of Clinical Oncology, The Affiliated Hospital of Xuzhou Medical University, Xuzhou, Jiangsu, China
[3]Jiangsu Center for the Collaboration and Innovation of Cancer Biotherapy, Xuzhou Medical University, Xuzhou, Jiangsu, China
[4]Clinical Laboratory, The Affiliated Huai'an Hospital of Xuzhou Medical University and Huai'an Second Hospital, Huai'an, Jiangsu, China
[5]Department of Oncology, Xuzhou Central Hospital, Xuzhou Clinical School of Xuzhou Medical University, Xuzhou, Jiangsu, China
[6]College of Life Sciences, Xuzhou Medical University, Xuzhou, Jiangsu, China
[7]Department of Medicine, Baylor College of Medicine, Houston, Texas, USA

Acknowledgements We thank Professor Lin Fang from Xuzhou Medical University for providing the plasmids and technical support. Schematic diagrams are created with BioRender.com.

Contributors DC, JZ, and RC: Conceived and designed the project. FZ, ZL, YZ, WT, GZ, YS, and BL: Performed the project and analyzed the data. JD, LF, HL, and GW: Contributed reagents, materials, and analysis tools. FZ and DC wrote, reviewed, and edited the manuscript. DC: Research guarantor. All the authors have read and approved the final manuscript.

Funding This project was supported by grants from the National Key R&D Program of China (2018YFA0900900), Natural Science Research of Jiangsu Higher Education Institutions of China (22KJA320004), National Natural Science Foundation of China (82072814), China Postdoctoral Science Foundation (2023M732974), Qing Lan Project of Jiangsu Province, Research Foundation of Xuzhou Medical University (D2022013), and Xuzhou Municipal Science and Technology Project (KC23038).

Competing interests None declared.

Patient consent for publication Not applicable.

Ethics approval All procedures and animal experimental protocols were approved by the Laboratory Animal Ethics Committee of Xuzhou Medical University.

Provenance and peer review Not commissioned; externally peer reviewed.

Data availability statement All data relevant to the study are included in the article or uploaded as supplementary information.

ORCID iDs
Gang Wang http://orcid.org/0000-0001-6020-7263
Junnian Zheng http://orcid.org/0000-0003-0208-6410
Dafei Chai http://orcid.org/0000-0002-8028-2954

REFERENCES

1 Xiao L, Yeung H, Haber M, *et al*. Immunometabolism: A "Hot" Switch for "Cold" Pediatric Solid Tumors. *Trends Cancer* 2021;7:751–77.
2 D'Alterio C, Scala S, Sozzi G, *et al*. Paradoxical effects of chemotherapy on tumor relapse and metastasis promotion. *Semin Cancer Biol* 2020;60:351–61.
3 Abel MK, Myers EL, Minkin E, *et al*. Cancer-directed surgery in patients with metastatic cancer: A systematic review and meta-analysis of randomized evidence. *Cancer Med* 2023;12:14072–83.
4 Comoli P, Chabannon C, Koehl U, *et al*. Development of adaptive immune effector therapies in solid tumors. *Ann Oncol* 2019;30:1740–50.
5 Zhang H, Liu L, Liu J, *et al*. Roles of tumor-associated macrophages in anti-PD-1/PD-L1 immunotherapy for solid cancers. *Mol Cancer* 2023;22:58.
6 Finck AV, Blanchard T, Roselle CP, *et al*. Engineered cellular immunotherapies in cancer and beyond. *Nat Med* 2022;28:678–89.
7 Harrington K, Freeman DJ, Kelly B, *et al*. Optimizing oncolytic virotherapy in cancer treatment. *Nat Rev Drug Discov* 2019;18:689–706.
8 Bjordahl R, Goulding J, Pribadi M, *et al*. Development of a Novel MICA/B-Specific CAR As a Pan-Tumor Targeting Strategy for Off-the-Shelf, Cell-Based Cancer Immunotherapy. *Blood* 2020;136:5–6.
9 Blass E, Ott PA. Advances in the development of personalized neoantigen-based therapeutic cancer vaccines. *Nat Rev Clin Oncol* 2021;18:215–29.
10 Lopes A, Vandermeulen G, Préat V. Cancer DNA vaccines: current preclinical and clinical developments and future perspectives. *J Exp Clin Cancer Res* 2019;38:146.
11 Zahm CD, Colluru VT, McNeel DG. DNA vaccines for prostate cancer. *Pharmacol Ther* 2017;174:27–42.
12 Hammerich L, Marron TU, Upadhyay R, *et al*. Systemic clinical tumor regressions and potentiation of PD1 blockade with in situ vaccination. *Nat Med* 2019;25:814–24.

13 Brody JD, Ai WZ, Czerwinski DK, *et al*. In situ vaccination with a TLR9 agonist induces systemic lymphoma regression: a phase I/II study. *J Clin Oncol* 2010;28:4324–32.
14 Kantoff PW, Higano CS, Shore ND, *et al*. Sipuleucel-T immunotherapy for castration-resistant prostate cancer. *N Engl J Med* 2010;363:411–22.
15 Cupovic J, Ring SS, Onder L, *et al*. Adenovirus vector vaccination reprograms pulmonary fibroblastic niches to support protective inflating memory CD8$^+$ T cells. *Nat Immunol* 2021;22:1042–51.
16 Tatsis N, Fitzgerald JC, Reyes-Sandoval A, *et al*. Adenoviral vectors persist in vivo and maintain activated CD8+ T cells: implications for their use as vaccines. *Blood* 2007;110:1916–23.
17 Chang J. Adenovirus Vectors: Excellent Tools for Vaccine Development. *Immune Netw* 2021;21:e6.
18 Barrera J, Brake DA, Kamicker BJ, *et al*. Safety profile of a replication-deficient human adenovirus-vectored foot-and-mouth disease virus serotype A24 subunit vaccine in cattle. *Transbound Emerg Dis* 2018;65:447–55.
19 Yan Y, Jing S, Feng L, *et al*. Construction and Characterization of a Novel Recombinant Attenuated and Replication-Deficient Candidate Human Adenovirus Type 3 Vaccine: "Adenovirus Vaccine Within an Adenovirus Vector." *Virol Sin* 2021;36:354–64.
20 Folegatti PM, Jenkin D, Morris S, *et al*. Vaccines based on the replication-deficient simian adenoviral vector ChAdOx1: Standardized template with key considerations for a risk/benefit assessment. *Vaccine (Auckl)* 2022;40:5248–62.
21 Andersen MH. Tumor microenvironment antigens. *Semin Immunopathol* 2023;45:253–64.
22 Leko V, Rosenberg SA. Identifying and Targeting Human Tumor Antigens for T Cell-Based Immunotherapy of Solid Tumors. *Cancer Cell* 2020;38:454–72.
23 Xu H, Zheng X, Zhang S, *et al*. Tumor antigens and immune subtypes guided mRNA vaccine development for kidney renal clear cell carcinoma. *Mol Cancer* 2021;20:159.
24 Sun S, Zhou W, Li X, *et al*. Nuclear Aurora kinase A triggers programmed death-ligand 1-mediated immune suppression by activating MYC transcription in triple-negative breast cancer. *Cancer Commun (Lond)* 2021;41:851–66.
25 Du R, Huang C, Liu K, *et al*. Targeting AURKA in Cancer: molecular mechanisms and opportunities for Cancer therapy. *Mol Cancer* 2021;20:15.
26 Casey NP, Fujiwara H, Tanimoto K, *et al*. A Functionally Superior Second-Generation Vector Expressing an Aurora Kinase-A-Specific T-Cell Receptor for Anti-Leukaemia Adoptive Immunotherapy. *PLoS One* 2016;11:e0156896.
27 Ochi T, Fujiwara H, Suemori K, *et al*. Aurora-A kinase: A novel target of cellular immunotherapy for leukemia. *Blood* 2009;113:66–74.
28 Ochi T, Fujiwara H, Yasukawa M. Aurora-A kinase: A novel target both for cellular immunotherapy and molecular target therapy against human leukemia. *Expert Opin Ther Targets* 2009;13:1399–410.
29 Wang-Bishop L, Chen Z, Gomaa A, *et al*. Inhibition of AURKA Reduces Proliferation and Survival of Gastrointestinal Cancer Cells With Activated KRAS by Preventing Activation of RPS6KB1. *Gastroenterology* 2019;156:662–75.
30 Nguyen TTT, Shang E, Shu C, *et al*. Aurora kinase A inhibition reverses the Warburg effect and elicits unique metabolic vulnerabilities in glioblastoma. *Nat Commun* 2021;12:5203.
31 Gong X, Du J, Parsons SH, *et al*. Aurora A Kinase Inhibition Is Synthetic Lethal with Loss of the *RB1* Tumor Suppressor Gene. *Cancer Discov* 2019;9:248–63.
32 Liang H, Du J, Elhassan RM, *et al*. Recent progress in development of cyclin-dependent kinase 7 inhibitors for cancer therapy. *Expert Opin Investig Drugs* 2021;30:61–76.
33 Yuan J, Li X, Yu S. CDK7-dependent transcriptional addiction in bone and soft tissue sarcomas: Present and Future. *Biochim Biophys Acta Rev Cancer* 2022;1877:188680.
34 Huang C-S, Xu Q-C, Dai C, *et al*. Nanomaterial-Facilitated Cyclin-Dependent Kinase 7 Inhibition Suppresses Gallbladder Cancer Progression via Targeting Transcriptional Addiction. *ACS Nano* 2021;15:14744–55.
35 Li Z-M, Liu G, Gao Y, *et al*. Targeting CDK7 in oncology: The avenue forward. *Pharmacol Ther* 2022;240:108229.
36 Wang J, Zhang R, Lin Z, *et al*. CDK7 inhibitor THZ1 enhances antiPD-1 therapy efficacy via the p38α/MYC/PD-L1 signaling in non-small cell lung cancer. *J Hematol Oncol* 2020;13:99.
37 Wei Y, Li C, Bian H, *et al*. Targeting CDK7 suppresses super enhancer-linked inflammatory genes and alleviates CAR T cell-induced cytokine release syndrome. *Mol Cancer* 2021;20:5.
38 Zeng S, Lan B, Ren X, *et al*. CDK7 inhibition augments response to multidrug chemotherapy in pancreatic cancer. *J Exp Clin Cancer Res* 2022;41:241.
39 Chow P-M, Liu S-H, Chang Y-W, *et al*. The covalent CDK7 inhibitor THZ1 enhances temsirolimus-induced cytotoxicity via autophagy suppression in human renal cell carcinoma. *Cancer Lett* 2020;471:27–37.
40 Rasool RU, Natesan R, Deng Q, *et al*. CDK7 Inhibition Suppresses Castration-Resistant Prostate Cancer through MED1 Inactivation. *Cancer Discov* 2019;9:1538–55.
41 Kim J, Cho Y-J, Ryu J-Y, *et al*. CDK7 is a reliable prognostic factor and novel therapeutic target in epithelial ovarian cancer. *Gynecol Oncol* 2020;156:211–21.
42 Kuempers C, Jagomast T, Heidel C, *et al*. CDK7 is a prognostic biomarker for non-small cell lung cancer. *Front Oncol* 2022;12:927140.
43 Liu J, Chen C, Wang D, *et al*. Emerging small-molecule inhibitors of the Bruton's tyrosine kinase (BTK): Current development. *Eur J Med Chem* 2021;217:113329.
44 Pal SK, He M, Tong T, *et al*. RNA-seq reveals aurora kinase-driven mTOR pathway activation in patients with sarcomatoid metastatic renal cell carcinoma. *Mol Cancer Res* 2015;13:130–7.
45 Miralaei N, Majd A, Ghaedi K, *et al*. Integrated pan-cancer of AURKA expression and drug sensitivity analysis reveals increased expression of AURKA is responsible for drug resistance. *Cancer Med* 2021;10:6428–41.
46 Pallasaho S, Gondane A, Kuivalainen A, *et al*. Castration-resistant prostate cancer cells are dependent on the high activity of CDK7. *J Cancer Res Clin Oncol* 2023;149:5255–63.
47 Wang C, Jin H, Gao D, *et al*. A CRISPR screen identifies CDK7 as a therapeutic target in hepatocellular carcinoma. *Cell Res* 2018;28:690–2.
48 Zhou Y, Lu L, Jiang G, *et al*. Targeting CDK7 increases the stability of Snail to promote the dissemination of colorectal cancer. *Cell Death Differ* 2019;26:1442–52.
49 Giovanelli P, Sandoval TA, Cubillos-Ruiz JR. Dendritic Cell Metabolism and Function in Tumors. *Trends Immunol* 2019;40:699–718.
50 Nguyen TL, Yin Y, Choi Y, *et al*. Enhanced Cancer DNA Vaccine *via* Direct Transfection to Host Dendritic Cells Recruited in Injectable Scaffolds. *ACS Nano* 2020;14:11623–36.
51 Jiang N, Zheng Y, Ding J, *et al*. The co-delivery of adenovirus-based immune checkpoint vaccine elicits a potent anti-tumor effect in renal carcinoma. *NPJ Vaccines* 2023;8:109.
52 Bae J, Kitayama S, Daheron L, *et al*. Rejuvenated BCMA-Specific CD8 + Cytotoxic T Lymphocytes Derived from Antigen-Specific Induced Pluripotent Stem Cells: Immunotherapeutic Application in Multiple Myeloma. *Blood* 2021;138:75.
53 Dudani S, de Velasco G, Wells JC, *et al*. Evaluation of Clear Cell, Papillary, and Chromophobe Renal Cell Carcinoma Metastasis Sites and Association With Survival. *JAMA Netw Open* 2021;4:e2021869.
54 Liu J, Fu M, Wang M, *et al*. Cancer vaccines as promising immuno-therapeutics: platforms and current progress. *J Hematol Oncol* 2022;15:28.
55 Saxena M, van der Burg SH, Melief CJM, *et al*. Therapeutic cancer vaccines. *Nat Rev Cancer* 2021;21:360–78.
56 Majhen D. Human adenovirus type 26 basic biology and its usage as vaccine vector. *Rev Med Virol* 2022;32:e2338.
57 Zhou X, Xiang Z, Ertl HCJ. Vaccine Design: Replication-Defective Adenovirus Vectors. *Methods Mol Biol* 2016;1404:329–49.
58 Catanzaro AT, Koup RA, Roederer M, *et al*. Phase 1 safety and immunogenicity evaluation of a multiclade HIV-1 candidate vaccine delivered by a replication-defective recombinant adenovirus vector. *J Infect Dis* 2006;194:1638–49.
59 Chen X, Ma J, Wang X, *et al*. *CCNB1* and *AURKA* are critical genes for prostate cancer progression and castration-resistant prostate cancer resistant to vinblastine. *Front Endocrinol (Lausanne)* 2022;13:1106175.
60 Zhong S, Zhang Y, Yin X, *et al*. CDK7 inhibitor suppresses tumor progression through blocking the cell cycle at the G2/M phase and inhibiting transcriptional activity in cervical cancer. *Onco Targets Ther* 2019;12:2137–47.
61 Cui C, Wang J, Fagerberg E, *et al*. Neoantigen-driven B cell and CD4T follicular helper cell collaboration promotes anti-tumor CD8 T cell responses. *Cell* 2021;184:6101–18.
62 Zander R, Schauder D, Xin G, *et al*. CD4+ T Cell Help Is Required for the Formation of a Cytolytic CD8+ T Cell Subset that Protects against Chronic Infection and Cancer. *Immunity* 2019;51:1028–42.
63 Graalmann T, Borst K, Manchanda H, *et al*. B cell depletion impairs vaccination-induced CD8$^+$ T cell responses in a type I interferon-dependent manner. *Ann Rheum Dis* 2021;80:1537–44.
64 Qin X, Yang T, Xu H, *et al*. Dying tumor cells-inspired vaccine for boosting humoral and cellular immunity against cancer. *J Control Release* 2023;359:359–72.